Faculty of Technology

PETROGRAPHIC CHARACTERIZATION OF EVAPORITES IN THE PETÄJÄSKOSKI FORMATION, PERÄPOHJA BELT, NORTHERN FINLAND.

Ummar Farid

International Master´s Programme: Mineral Resources and Sustainable Mining

Oulu Mining School

Master's Thesis

June 2022

International Maters Program in geosciences Mineral Resources and Sustainable Mining	
Author Ummar Farid	Thesis Supervisor Jukka-Pekka Ranta, Kari Strand

Title of Thesis

PETROGRAPHIC CHARACTERIZATION OF EVAPORITES IN THE PETÄJÄSKOSKI FORMATION, PERÄPOHJA BELT, NORTHERN FINLAND.

	Type of Thesis	Submission date	No of pages
	Master's Thesis	23 June 2022	52

Abstract

The present study aims to characterize the Petäjäskoski formation in the Paleoproterozoic Peräpohja belt, and to identify the evaporite sequence through petrographic and electron microprobe analysis. The Peräpohja belt in northwestern Finland is known to host for example atypical orogenic Gold (Au)-Cobalt (Co)-Uranium(U) deposits of Rompas-Rajapalot, where evaporites have shown to play a major role in formation of these deposits. Evaporites have also important part in the genesis of various deposits worldwide, including Iron Oxide Copper Deposit (IOCG) and Sediment hosted stratiform (SSC). In order to comprehend the source of the salt rich solutions and rock types, drill core samples from Petäjäskoski were examined through petrographic and electron microprobe studies.

Petrographic studies shows the major lithologies as a mudstone-sandstone-dolomite unit with collapsed breccias. Mudstones contains fine and dark layers with quartz, feldspar, muscovite, and sericite. Sandstone is recrystallized as well as well-rounded sub arkose units with quartz, plagioclase, orthoclase, microcline, biotite, muscovite and trace zircon and hematite. Dolomite is recrystallized and talc rich while conglomerate is monomictic with mudstone clast and quartz, feldspars, and talc as major minerals.

Microprobe analysis of selected samples showed in accessory halite, anhydrite, sylvite and bischofite which are supporting the evaporitic origin the Petäjäskoski formation. Stromatolitic dolomite, flaser and lenticular bedded mudstone, brecciated unit, anhydrite pseudomorphs, and fractures filled with calcite pseudomorphs after evaporite minerals suggests shallow ramp tidal flat/lagoonal depositional condition, where conditions were suitable for evaporite sedimentation. Further support is indicated by collapse breccias within the formation making these rocks oldest evaporitic rocks in the Fennoscandian shield.

Table of Contents

1. Introduction

The Paleoproterozoic supracrustal rocks of the Peräpohja belt in Northern Finland host several orogenic gold deposits with atypical metal association such as Rompas-Rajapalot Au-Co, and Kivimaa Au-Cu deposits where gold is associated with copper (Cu), cobalt (Co) uranium (U), and antimony (Sb) in metamorphosed sedimentary and volcanic rocks (Molnár et al., 2016; Ranta et al., 2018). The enrichment of base metals along with gold in seemingly orogenic type of gold deposit is a controversy, as the relatively reduced orogenic fluids are not able to carry significant amount of base metals, due to the lack of chloride which is the main ligand to carry e.g., Co and Cu in hydrothermal fluids (Davey, 2019; Vasilopoulos et al., 2021). One of proposed requirement for the formation of these atypical orogenic gold deposits is presence of basinal brines/salt rich solutions that selectively leach, carry and precipitates base metals at low temperatures, through hydrothermal alteration in fractures and fissures of country rock prior to the orogenic processes. Evaporites are potential source for saline basinal brines with fluids rich in chloride. (Rose, 1976; Warren, 2016). Several other ore deposits types such as Iron Oxide Copper Gold (IOCG) of Humboldt complex (USA), Korshunovsk and Tagar (Russia), Olympic dam (Australia) and stratiform Copper-Cobalt-Silver deposits of Central African copper belt have been linked with evaporites (Pirajno, 2009). In addition to the capability of evaporitic fluids to transport metals, interaction with S-rich evaporitic beds (anhydrite) with sulphur poor mafic-ultramafic magmas provide sulphur and can lead to the formation of large-scale Ni-Cu-PGM sulphide deposits such as Norilsk's Russia (Warren, 2016).

Evidence for existence of evaporitic strata in the Paleoproterozoic supracrustal units in northern Finland is being discussed by several workers during the recent decades (e.g., Ranta et al., 2018; Haverinen et al., 2020). Based on inferred collapse breccias in Kuusamo belt, presence of gypsum and anhydrite in Central Lapland belt (CLB) (Haverinen, 2020), inferred collapsed breccias and thick anhydrite beds within Peräpohja belt in the (Kyläkoski et al., 2012; Tapio et al., 2021), as well as extensive albitization, tourmalinization, and scapolitization in Paleoproterozoic rocks which are an indirect evidence of possible evaporites in northern Finland.

The present study aims to study 16 samples of three drill cores from the Paleoproterozoic Petäjäskoski formation in Peräpohja belt to better understand and characterize the Petäjäskoski formation itself and to interpret the existence of evaporites in the Petäjäskoski formation. This

work is a complementary to pioneering work of Kyläkoski et al. (2012) who first described this unusual lithological association within the Peräpohja belt.

The petrographic study was carried out to characterize the rock types, mineralogy and especially detection of minerals related to the evaporitic environment, while electron microprobe analysis was performed to conform and obtained chemical composition of evaporite minerals in order to better comprehend the genesis of ore formation processes in the Peräpohja belt.

2. Regional geological setting

In northwestern Finland, the Paleoproterozoic Peräpohja belt (PB) is a demonstration of intra-continental failed pull apart basin (aulacogen) overlying the Archean basement rocks (Fig. 1; Kyläkoski et al., 2012; Molnár et al., 2016). Geographical distribution of the Peräpohja belt encompasses the municipalities of Kemi, Tornio, Keminmaa, Yliotornio, Simo, Ranua and Rovaniemi and is 80km wide and 170km long triangular shaped belt. The depositional span of Peräpohja belt is ca. 600 Myr starting after 2.44 Ga which is recorded age of underlying basement layered mafic-ultramafic complexes, with deposition of Palokivalo at 2.2 Ga until ca. 1.88 Ga which is reportedly the age of Haaparanta suite monzonite dikes which cuts the pelitic metasediment of the basin (Iljina and Hanski, 2005; Ranta et al., 2015 ; Tapio et al., 2021). The rocks of Peräpohja belt have a stratigraphic thickness of 5 km with thin-skinned deformation consist of large synclinorium suggested by geophysical studies and consist of quartzites, intrusive, volcaniclastics, mafic volcanics, carbonates, black shales, greywackes, and mica schist and have various base metals and gold mineralization and prospects (Kyläkoski et al., 2012; Lahtinen et al., 2019). In the north and east boundary of the Peräpohja belt with granitoids of Paleoproterozoic Central Lapland granitoid complex (CLGC) is tectonic-metamorphic (Tapio et al., 2021). In south, the Peräpohja belt is bounded by basement rocks of Archean Pudasjarvi complex which is being intruded by mafic-ultramafic layered intrusions of Portimo, Penikat and Kemi (Molnár et al., 2016). The N-S trending Pajala shear zone close to the Tornionjoki river is western boundary between the Peräpohja belt and the Norbotten craton in Sweden (Ranta et al., 2015; Molnár et al., 2016).

Basin development in the Peräpohja belt starts with rifting of basement. Basin evolution for the Peräpohja, Central Lapland and Kuusamo belts were developed in five different stages from 2.5-1.88 Ga, based on zircon morphology, whole-rock geochemistry, geochronological data, and field

experience as **a)** early rift/initial rifting, **b)** syn rift stage, **c)** syn-early post rift. These periods were characterized by both marine and continental sediment deposition along with subaqueous and subaerial volcanism followed by evaporite and carbonate sedimentation suggesting as a result of tectonic stability. **d)** A passive margin stage lasting from 2.1-1.94-1.92 Ga is time of aulacogen development, where deposition is mostly hemipelagic, gravity flows sandstone, and oceanic volcanism**. e)** the last is compressional stage where forebulge and magmatic arc collision takes place and subsequently basin inversion forming a fold and thrust belt and related foreland deposits (Köykkä et al., 2019; Tapio et al., 2021).

The grade of metamorphism and tectonism varied across the Peräpohja belt. In north and north-east rocks have undergone amphibolite facies metamorphism whereas in south rocks have greenschist facies metamorphism, with primary features being well-preserved (Hölttä et al., 2017; Ranta et al., 2018). Several deformation events and related metamorphism have occurred due to Svecofennian orogeny (1.9-1.8 Ga) including late-stage orogenic granites in Central Lapland granitoid complex from 1.84-1.80 Ga. The migmatization of pelitic sediments in northern tectonized boundary between Peräpohja belt and Central Lapland granitoid complex is another deformation event with age of ca. 1.8 Ga (Ranta et al., 2015).

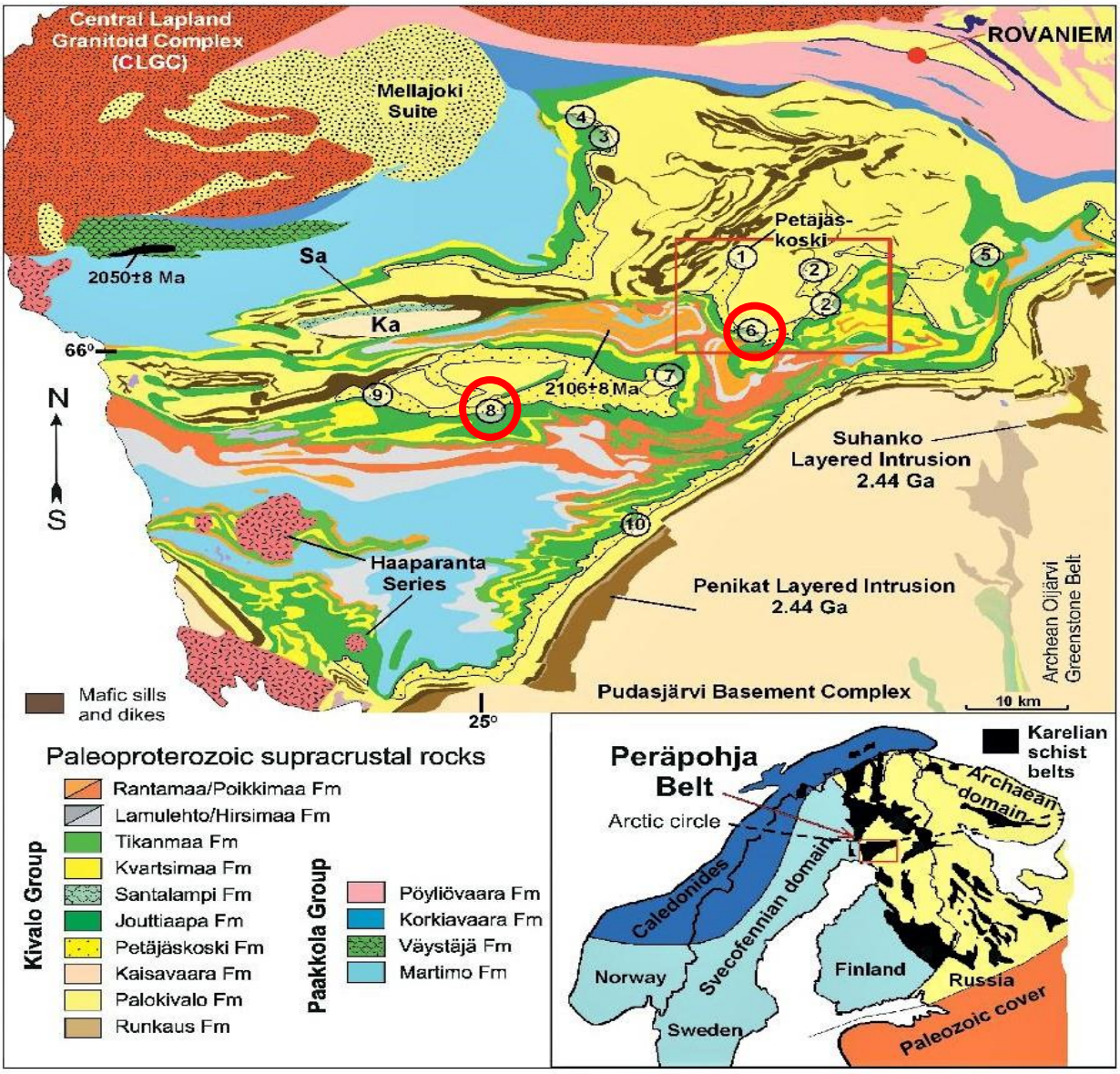

Figure 1. Stratigraphic map and location of Peräpohja belt, 6 and 8 are drill hole sites for present study after (Kyläkoski et al., 2012). Published with an permission of Bulletin of the Geological Society of Finland.

3. Stratigraphy of Peräpohja belt

Supracrustal rock units of the Peräpohja belt comprises of two main lithostratigraphic groups, the Kivalo and Paakkola (Table 1) which previously were classified as being Jatulian and Kalevian formations respectively (Hanski et al., 2005; Ranta et al., 2015).

Sompujärvi formation

The 50-meter thick Sompujärvi formation in south-east of basin forms the basal stratigraphic unit of Peräpohja belt, sitting on top of mafic and ultramafic intrusions of platinum earth elements (PGE) potential and Archean Pudasjärvi complex (Iljina and Hanski, 2005; Kyläkoski et al., 2012; Piippo et al., 2019). The lithologies includes polymictic conglomerates where pebbles originating from layered intrusives, granites and plutonic rocks, arkoses, and quartzite. The presence of conglomerates on top of intrusive layered complex suggests uplifting of crust and erosion followed by magmatism (Kyläkoski et al., 2012; Melezhik et al., 2012).

Runkaus Formation

The Runkaus formation occurs near the Archean Proterozoic boundary. It is representation of mafic volcanic rocks (Hanski, 2003). The thickness is 10-200m and rocks are subaerial amygdaloidal basalt flows and agglomerates with secondary titanite U-Pb age of 2250 Ma (Kyläkoski et al., 2012; Huhma et al., 1990).

Palokivalo Formation

The Palokivalo formation is composed of arenites and quartzites of 1 km in total thickness, showing with ripple marks and desiccation/mud cracks. The mud cracks in shale, wave and current ripples in sandstone suggests shallow marine depositional conditions *(*cf. Kyläkoski et al., 2012). These arenites and quartzites have been intruded by mafic sills of ca. 2220 Ma thus suggesting the age of Palokivalo formation as 2.22 Ga (Hanski et al., 2010).

Petäjäskoski Formation

Detailed description of the Petäjäskoski formation was postulated by (Kyläkoski et al., 2012) which previously was classified to be part of the Palokivalo formation. Petäjäskoski formation has no natural exposures and is only outcropped along the banks of Petäjäskoski water channel where due to prolong long contact with water and air, the rocks are badly weathered. The contact with with the Palokivalo formation is intersected in the drillholes. Petäjäskoski formation have strong electromagnetic and low gravity anomaly because of weathered crust and wet overburden, which shows its basin wide presence in the Peräpohja belt. It is exposed in the Petäjäskoski electric-power plant channel where rocks are folded, weathered, and discontinuous. The main lithologies are

mudstone, siltstone (micaceous schist), quartzite, and dolomite. The sedimentary structures include flaser, lenticular bedding and rhythmites in mudstone and siltstone, cross bedding in sandstone, and stromatolites in dolomite. The age assigned to this formation is between 2220 and 2140 Ma based on U-Pb zircon age dating of mafic sills intruding the Petäjäskoski formation (Kyläkoski et al., 2012). Sedimentary structures formed by oscillatory flow conditions suggested by bidirectional cross bedding in sandstone, mud cracks and drapes in mudstone, stromatolites in dolomite along with siliciclastic and carbonate sequence suggest deposition in fluctuating subaerial and shallow water conditions in tidal flats environment where conditions for formation of evaporite were favorable during sometime (Kyläkoski et al., 2012).

Jouttiaapa formation

The Petäjäskoski formation is overlaid by the subaerially erupted tholeiitic Jouttiaapa basalts of ca. 2105±50 Ma with thickness of 300-1000m (Piippo et al., 2019). These continental flood basalts are enriched in PGE. The stratigraphic position of Santalampi formation pillowed and pyroclastic basalts and Kaisavaara formation quartzites is ambiguous and correlated as part of the Jouttiaapa and Palokivalo formations, respectively (Köykkä et al., 2019).

Kvartsimaa formation

The Kvartsimaa formation lies unconformably over the Jouttiaapa basalts and composed mainly of orthoquartzites. Sedimentary structures like cross bedding and ripples marks are common features in more impure quartzites. Occasionally dolomitic stromatolites are also present in the Kvartsimaa formation (Piippo et al., 2019; Köykkä et al., 2019).

Hirsimaa, and Tikanmaa formation

The Hirsimaa formation is comprised of fine grained mafic tuffite, with high magnetic susceptibility and thickness of 100-400m. the age of this formation is 2106±8 Ma as result of U-Pb age dating on zircons (Karhu et al., 2007). The lithology of the Tikanmaa formation is fine grained green mafic tuffites, 200-300m thick and present in some places across basin. The mineralogy is chlorite, actinolite, epidote and albite.

Rantamaa and Poikkimaa formations

The Rantamaa formation consist of stromatolitic dolomite, with thickness of 100-300m. Desiccation cracks, ripple marks and herringbone cross stratification is common structures in dolomite bearing quartzite (Perttunen and Hanski 2003). The dolomites of Rantamaa formation also have positive mean ^{13}C value of 10.7±0.8%, suggesting increased organic matter burial and rise in atmospheric oxygen at that time (Karhu, 1993). The Poikkimaa formation is non-magnetic susceptibility fine grained dolomite, magnetically distinctive from the associated Rantamaa and Hirsimaa formations. Petrographically the Poikkimaa formation is analogous to the Rantamaa's dolomite (Köykkä et al., 2019).

Lithodemic Units

The upper stratigraphy of Peräpohja belt is recently categorized as non-stratified lithodemic units (Lahtinen et al., 2015, 2019). Previously the upper part was classified as the Paakkola group including the Väystäjä, Korkiavaara and Pöyliövaara formations (Ranta et al., 2015). Currently, the Liekopalo and Kaskimaa formations are considered as part of the Kaskimaa greywackes of the Martimo suite and Ristivuoma formation is part of the Uusivirka suite (Lahtinen et al., 2015).

The Mellajoki suite located at northern part of Peräpohja belt is made up of deformed mica schists, quartzites and gneisses and can be related with the quartzites of Palokivalo formation (Hanski, 2003; Ranta et al., 2015). These rocks are intruded by calc-alkaline Kierovaara granites 1989 ± 6 Ma, that represent episode of felsic plutonism during late-stage deposition of karelian volcano-sedimentary sequence, in northern Finland. These are similar in age with Korkiavaara rocks having A-type signature ((Hanski et al., 2005); Ranta et al., 2015).

The Liekopalo formation comprises of paraschist containing iron sulphide and graphite with local interlayers of quartzite and can be correlated with quartzites of the Palokivalo in south-east and Mellajoki suite in north where it has brecciated contact. The Kaskimaa greywacke is a turbidite sequence showing evidence of deepening ocean basin, having source from both quartzites and volacanic rocks (Lahtinen et al., 2015). The Väystäjä suite is categorized in to three rock units with two lower mafic rocks and an upper sedimentary unit. The lower mafic rock unit of Väystäjä suite's has an upper age limit of 2084±11 Ma (Huhma et al., 2018) while upper mafic unit is associated with intraformational conglomerates, dolomite, volcano-sedimentary rocks and porphyries with upper age bracket of 2.09-2.05 Ga (Lahtinen et al., 2015). The

sedimentary unit of Väystäjä suite is made up of paraschists and pyrrhotite rich phyllites with 1-5 cm thick layers and interlayers of mafic volcanic (Lahtinen et al., 2015; Piippo et al., 2019).

The Rovaniemi supersuite which includes Hosiojoki, Rovajärvi and Oikarila formations are composed up of paragneisses, quartzites and paraschist and arkosic quartzites where sediments were derived from rift passive margin environment and angular zircon morphologies from these sediments suggests little transport and rapid sedimentation (Köykkä et al., 2019).

The Ristivuoma formation is syn-collisional forming during the early phase of foreland basin developement and contains paraschists, with thin layers of phyllite with more felsic source from the Paleoproterozoic granitoids (Köykkä et al., 2019).

Table 1. Lithostratigraphic column of Peräpohja belt after (Köykkä et al., 2019 and references therein;).

Group	Formation/ Lithodeme	Lithology	Age
Uusivirka	Ristivuoma	Paraschist	<1.92 Ga
Kierovaara	Kierovaara	Porphyritic granitic gneiss	1.9 Ga
Hosiojoki	Hosiojoki	Quartz-feldspar gneiss	<1.97 Ga
Martimo	Kaskimaa	Greywacke	<1.99/<2.10 Ga?
	Upper Västäja	Volcano-sedimentary	>2.05 Ga
	Lower Västäja	Metavolcanic rock	>2.08 Ga
	Västäja	Phyllites and Paraschist	
	Liekopalo	Paraschist	<2.65 Ga
Kivalo	Lehmulehto	Maffic tuffite	
	Rantamaa	Dolomite-quartzite	<2.65 Ga
	Hirsimaa	Mafic tuffite	2.1 Ga
	Poikkimaa	Dolomite-Phyllite	<2.13 Ga
	Tikanmaa	Mafic tuffite	
	Kvartsimaa	Quartzite-Dolomite	<2.65 Ga
	Santalampi	Agglomerate, Pillow basalt	
	Jouttiaapa	Amygdaloidal basalt	2.14 Ga
	Petäjäskoski	Mica-albite schist, dolomite,	<2.65 Ga
	Kaisavaara	Quartzite, conglomerate	
	Palokivalo and Mellajoki suite	Quartzite, orthoquartzite, mica gneiss, mica schist	<2.64 Ga and <2.36 Ga
	Runkaus	Amygdaloidal basalt, agglomerate	>2.25 Ga
	Sompujarvi	Conglomerate, Arkose, quartzite	

4. Evaporites and their role in Ore deposit Formation

Evaporites are sedimentary rocks formed in a restricted basin from salt enriched (brine) water body where evaporation exceeds the influx of water from rivers or streams usually known as "evaporating dish" process (Selley, 2000). In order to form evaporite deposits, three conditions are required, **a)** a salt rich water body at or close to surface, in arid-semiarid climate where salt can be precipitated with hydrological characters that enables adequate brine containing water at or close to surface, **b)** enough space available in sedimentary basin not occupied by other sediments, **c)** preserving burial environment where porewater cannot dissolve the deposited salts (Warren, 2016). Evaporite have played a major role in accumulation of ore deposits, as it increases the ore volume by making a transport/carrier system for metals and allow the concentrated precipitation of ore minerals. One such example is Noril'sk Ni-Cu of Siberia and Muruntau gold deposit in Uzbekistan (Wilde et al., 2001; Li et al., 2009). Evaporite-magma interaction take place in two forms either as orthomagmatic and paramagmatic. Orthomagmatic deposits may/maynot be associated with magma-evaporites interaction but when it does so it involves the incorporation of anhydrite bearing rocks into magmatic body before solidification, where sulfur is provided by these evaporites and originally sulfur undersaturated komatiitic and picritic melt (Keays, 1995) becomes saturated forming Ni-Cu and PGE ore deposits which otherwise won't be possible without external sulfur. Nickel and copper reserves of Noril'sk deposit is much higher than Sudbury and Jinchaun because of its association with assimilation of sulphates bearing evaporites. Paramagmatic ore deposits developed outside of magma as hydrothermal alteration products due to basinal brines/country rock reaction/interaction with fluids and solutions derived from magma (Warren, 2016). Several IOCG (Iron Oxide Copper Gold) deposit, e.g. Olympic dam ore formation have been attributed to the hot fluids convection due to magmatic heat that dissolves evaporites especially if halite is present, generating abundant amount of chloride which can transport and leach Copper (Cu), Gold (Au), lead (Pb), Iron (Fe), Zinc (Zn) in form of chloride complexes with deposition in pore spaces, fissures or fractures and abundant albitization of country rocks (McPhie et al., 2011).

5. Sampling and analytical methods

a. *Sampling*

Samples were collected from the drill cores intersecting the Petäjäskoski formation at the core facility of Palsatech Oy (Table 2). The two drillholes R104 and R105 were drilled in 2005 (Fig. 2; 3) and drill hole R521(Fig. 4) in 1994 by GTK in southern Peräpohja belt well before recognition of Petäjäskoski as formation. Along with sample collection these drillholes were studied in terms of textures, sedimentary structures, alterations and lithologies. The length of R105 is 150m while R521 is 307.80m thick. The total of 15 representative samples from various lithologies of the Petäjäskoski formation were collected for petrographic studies.

Table 2. List of samples collected from the Petäjäskoski drill cores.

	Drillhole ID	Sample ID	Lithology
1	R105	63.90m	Mudstone
2	R105	70.25m	Fine-grained Mudstone with dark and light layers
3	R105	144.20m	Breccia with clast of various sizes
4	R521	131.20m	Oxidized Mudstone
5	R521	191.60m	Chlorite rich Sandstone
6	R521	193m	Altered Sandstone
7	R521	196.20m	Dolomite
8	R521	215.20m	Sandstone
9	R521	221.50m	Sandstone
10	R521	233.46m	Grey sandstone with visible calcite vein fillings
11	R521	234.70m	Grey altered Sandstone
12	R521	240.47m	Sandstone
13	R521	241.55m	Altered Sandstone
14	R521	241.60m	Coarse grained Sandstone
15	R521	244m	Coarse grained Sandstone
16	R521	261.97m	Sandstone with visible layering

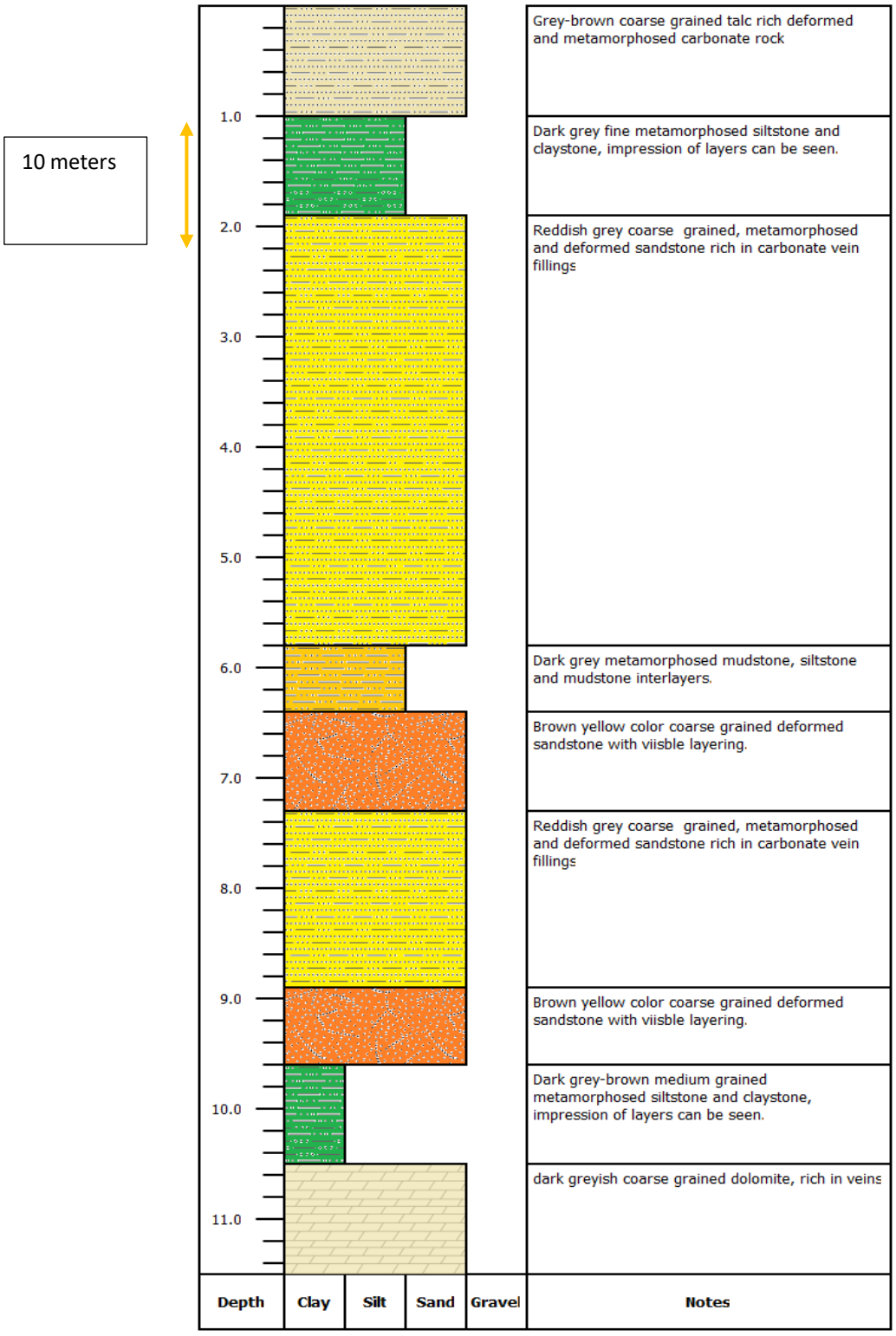

Figure 2. Drill core log of R104 from the Petäjäskoski formation each bar represents 10 meters, while upper 25m is regolith.

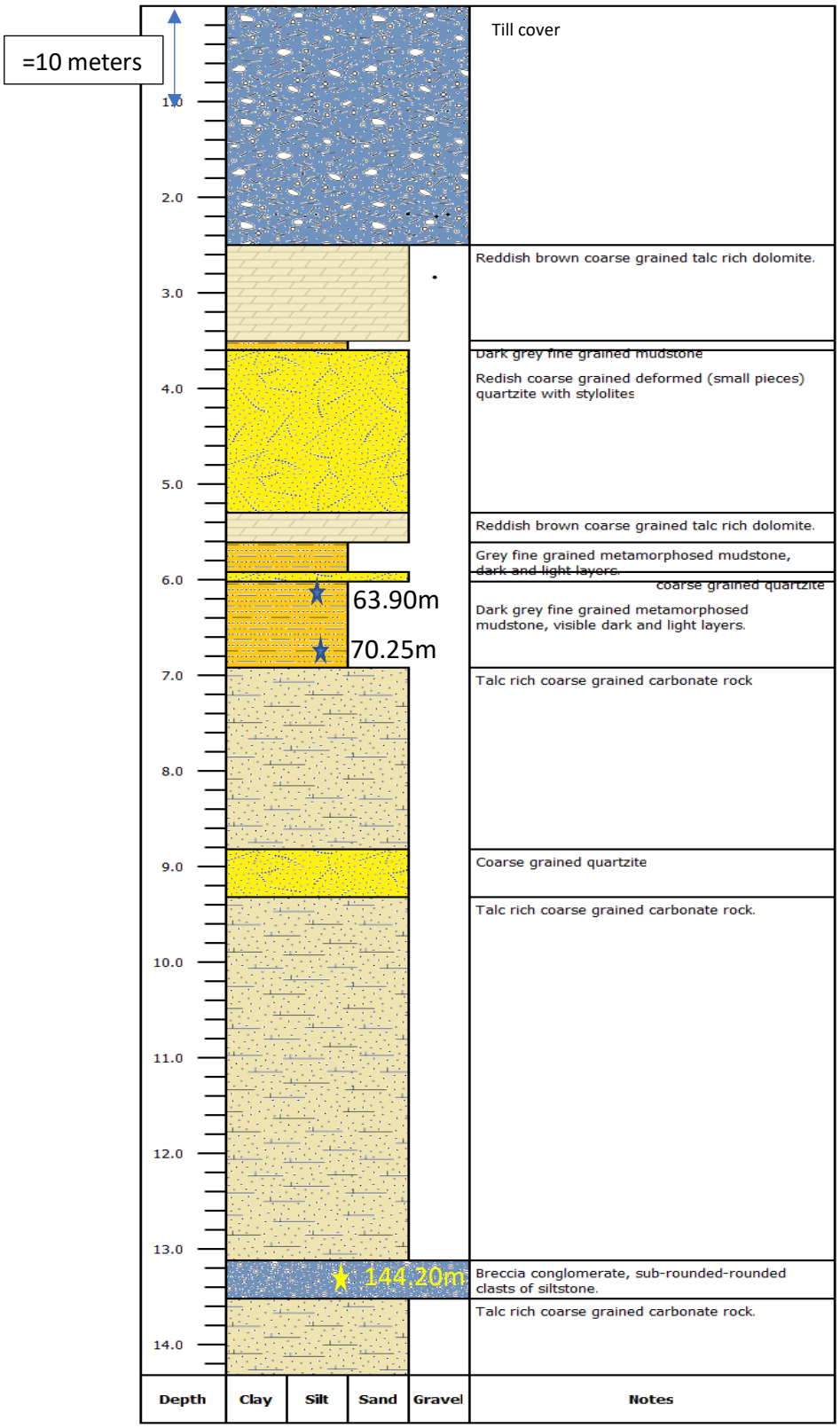

Figure 3. Drill core log of R105 from the Petäjäskoski formation, 150m thick.

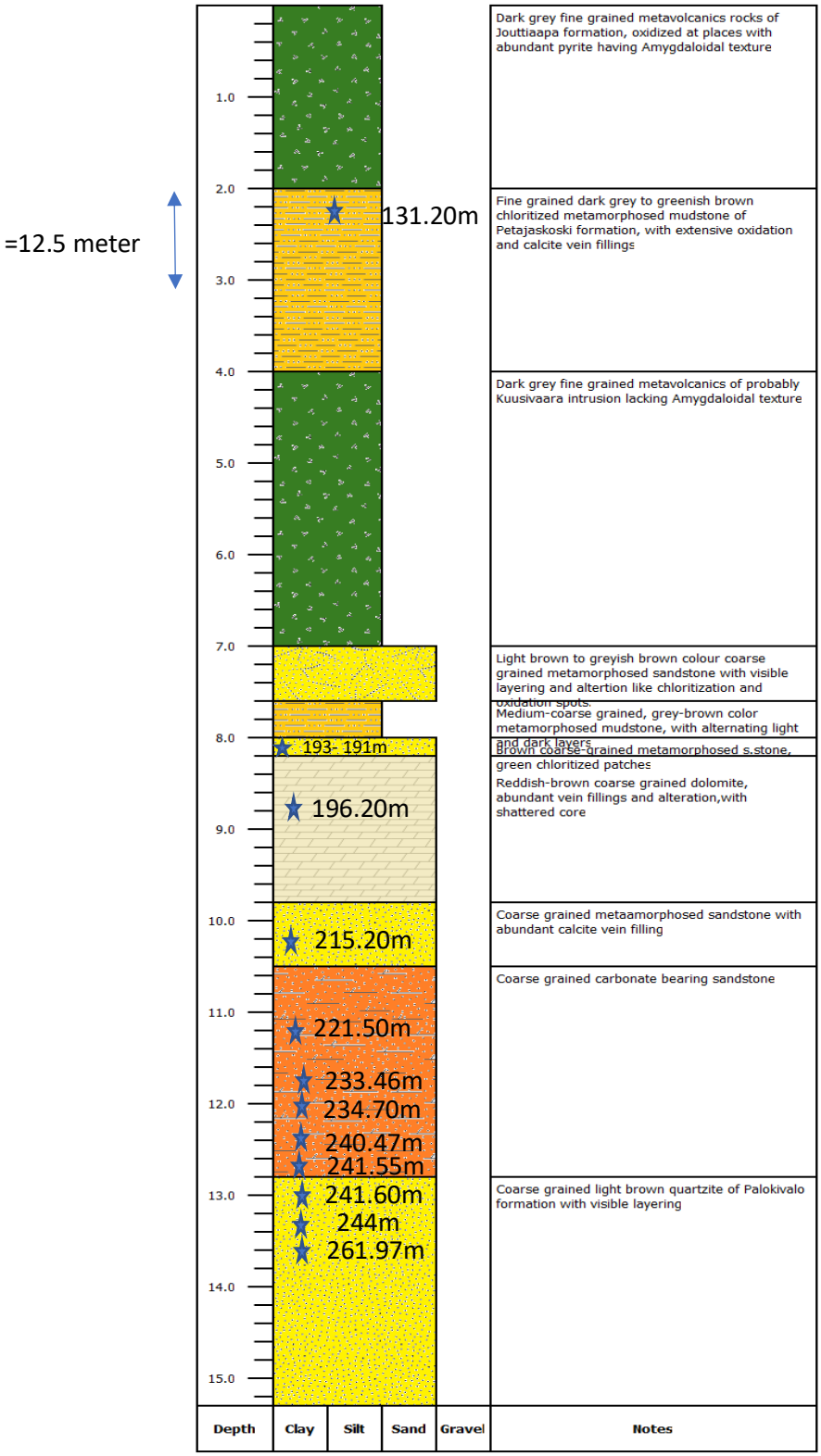

Figure 4. Drill core log R521 R521of the Palokivalo, Petäjäskoski and Jouttiaapa formations each bar is 12.5 meters excluding the Jouttiaapa formation.

b. *Petrography*

Polished thin sections were prepared in the Oulu Mining School thin section laboratory. The thin sections were studied under transmitted-reflected light Leica DM750P microscope. Thin section photographs were captured by Zeiss-Axioplan microscope equipped with a camera of Axiocam 105 supported by Zen2 core computer software.

c. *Electron Microprobe*

Electron Microprobe analysis of selected samples were studied at the Centre for Material Analysis (CMA), at University of Oulu. Analysis was performed with JEOL JXA 8200 electron microprobe with current beam of 10 nA and voltage of 15kV which is found to be favorable for studying e.g., sulfate minerals. The Energy dispersive spectrometer (EDS) was mainly used for determining mineral composition because small crystals/grains of halite will be destroyed by using Wavelength dispersive spectrometer (WDS). Only for one sample of anhydrite WDS was used.

6.1 Petrography

6.1.1 Mudstone

Mudstone samples are purple-light greenish in appearance with visible carbonate alteration. The laminas are thin dark claystone and coarse light color siltstone interlayers commonly few cm's thick, collectively called as mudstone. Small-scale cross bedding is not observed in drill sections of mudstone (cf. Kyläkoski et al., 2012) though flaser, lenticular bedding, and syn-sedimentary deformation as folding of layers is evident (Fig. 5). Calcite "rosette" or rosette aggregates are present in mudstone and are typical radiating rose like laths of originally gypsum/anhydrite which later are dissolved/leached and replaced by calcite during evaporite calcitization, while preserving their original texture. These are typical features suggesting early existence of evaporite in a rock (Fig. 6a). In mudstone sample (Fig. 7a) distinctive fractures can be seen which is now filled with calcite is another evidence of dissolution of older evaporitic intercalations.

Petrographic results of mudstones show alternate fine grained dark and lighter coarse-grained layers known as rhythmites, the evidence of seasonal deposition (Fig. 6b and 7b). The light layer contains mainly quartz, feldspar and phlogopite while dark layers made up of opaque mineral and organic matter. The quartz is fine grained fractured, subrounded-angular faces with undulose

extinction (Fig. 6d-e, and 7c, f). Feldspar occurs as subrounded grains of plagioclase (Albite) and Alkali feldspar (Microcline) with typical simple, tartan/gridlike and polysynthetic twinning is second most abundant mineral after quartz (Fig. 6d-e and 7d-g). Sericite the common alteration product of feldspar, is found both within plagioclase and microcline grains and on boundaries/contacts, shows severe alteration of feldspars. Mica includes muscovite and sericite make up the third largest concentration in mudstones with typical laths/flaky grains often fan like growth and are larger in grain size than quartz and felspar (Fig. 6c-d, Fig. 7c-d). The fine fraction of mudstone is composed up of fine-grained quartz, chlorite, opaque minerals, argillaceous and organic matter.

Figure 5. Photograph of drillcore showing flaser (individual mud drapes) and lenticular bedding (rippled silt) in mudstone although layers are syn-sedimentary folded, still recognizable.

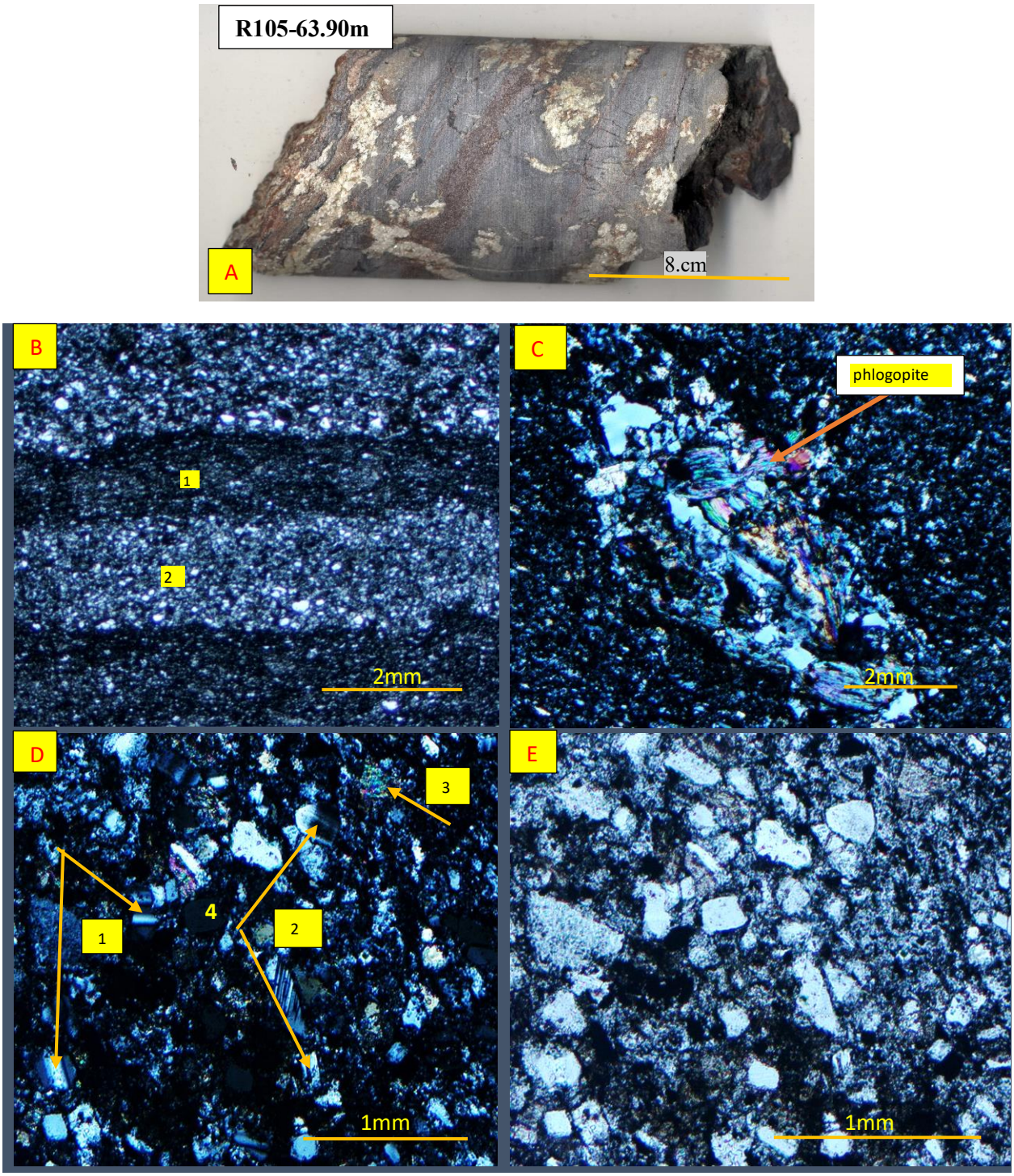

Figure 6. A) Drill core sample R105-63.90 fine grained mudstone with altered visible alternate dark (muddy) and light (silty) layers. **B)** photomicrographs showing alternate fine dark mud (1) and coarse lighter color more silty (2) layers PPL. **C)** Phlogopite and fine sericite matrix in alteration zone. **D)** 1 zoom in view of light layers, shows plagioclase feldspar's simple and polysynthetic twinning and 2 shows microcline in argillaceous matter cross polarized light, 3 is muscovite and 4 is quartz, XPL. **E)** Same view in Plane polarized light, PPL.

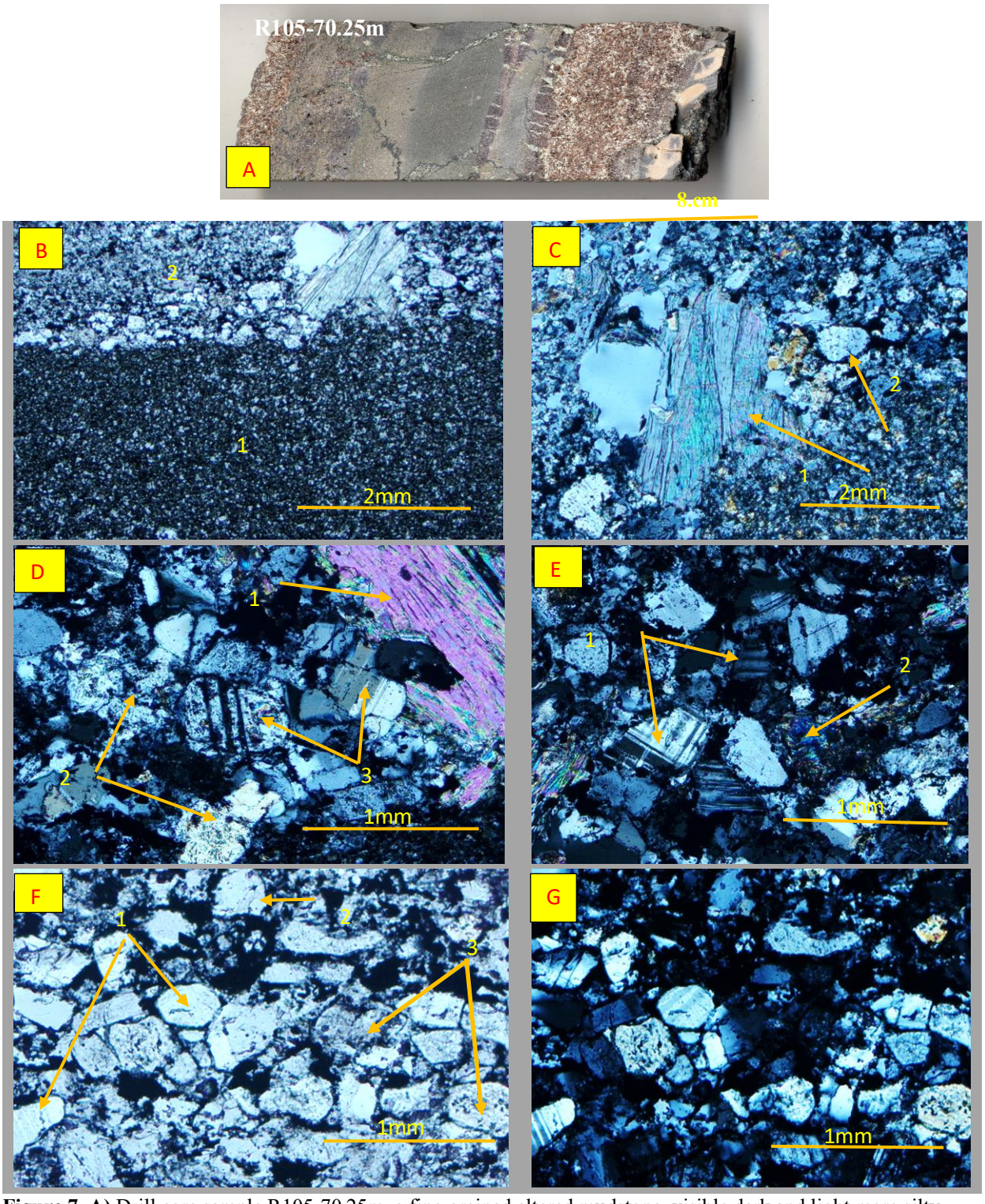

Figure 7. **A)** Drill core sample R105-70.25m, a fine-grained altered mudstone, visible dark and light more silty layers. **B)** 1 is fine grained mud with argillic content (PPL) and 2 is coarse grained quartz, feldspar, and phlogopite. **C)** 1is sheet like phlogopite and 2 is quartz (XPL) **D)** 1 is talc, 2 is k-feldspar, orthoclase, while 3 is plagioclase with visible twin planes and alteration to sericite (XPL). **E)** 1 is microcline with gridlike twinning and 2 is fine grained muscovite. **F)** 1 is plagioclase, 2 is quartz ($Q_{m)}$ and 3 is K-feldspar, dark material is argillaceous material. (PPl) **G)** same photo in XPL.

6.1.2 Chloritized mudstone

The sample 131.30m occurs at the top portion of R521 drill core (Fig. 8a). The major mineral composition of this sample is comprised of quartz, chlorite, opaque minerals, epidote, and calcite. Abundant chloritization is characteristics of this rock constituting about 30% of whole rock, chlorite is prismatic to massive in appearance, possibly the product of hydrothermal alteration of biotite or as precipitation from solutions in veins. Quartz grains are monocrystalline often fractured and distorted making up 25% (Fig. 8b-d). Opaque mineral is hexagonal shape pyrite present in immense amount about 15% of total rock (Fig. 8d). Epidote is also present, and some epidote grains are also zoned with tabular to well-developed pseudo-hexagonal grains and constitute about 15% of whole rock composition (Fig. 8b-d). The remaining is calcite which is present as large grains and often altered by chloritization where middle of calcite grains is replaced by chlorite grains (Fig. 8e). This sample represents an alteration horizon between less weathered rocks and distinctive in appearance both in hand specimen and in thin section as compared to adjacent rock units.

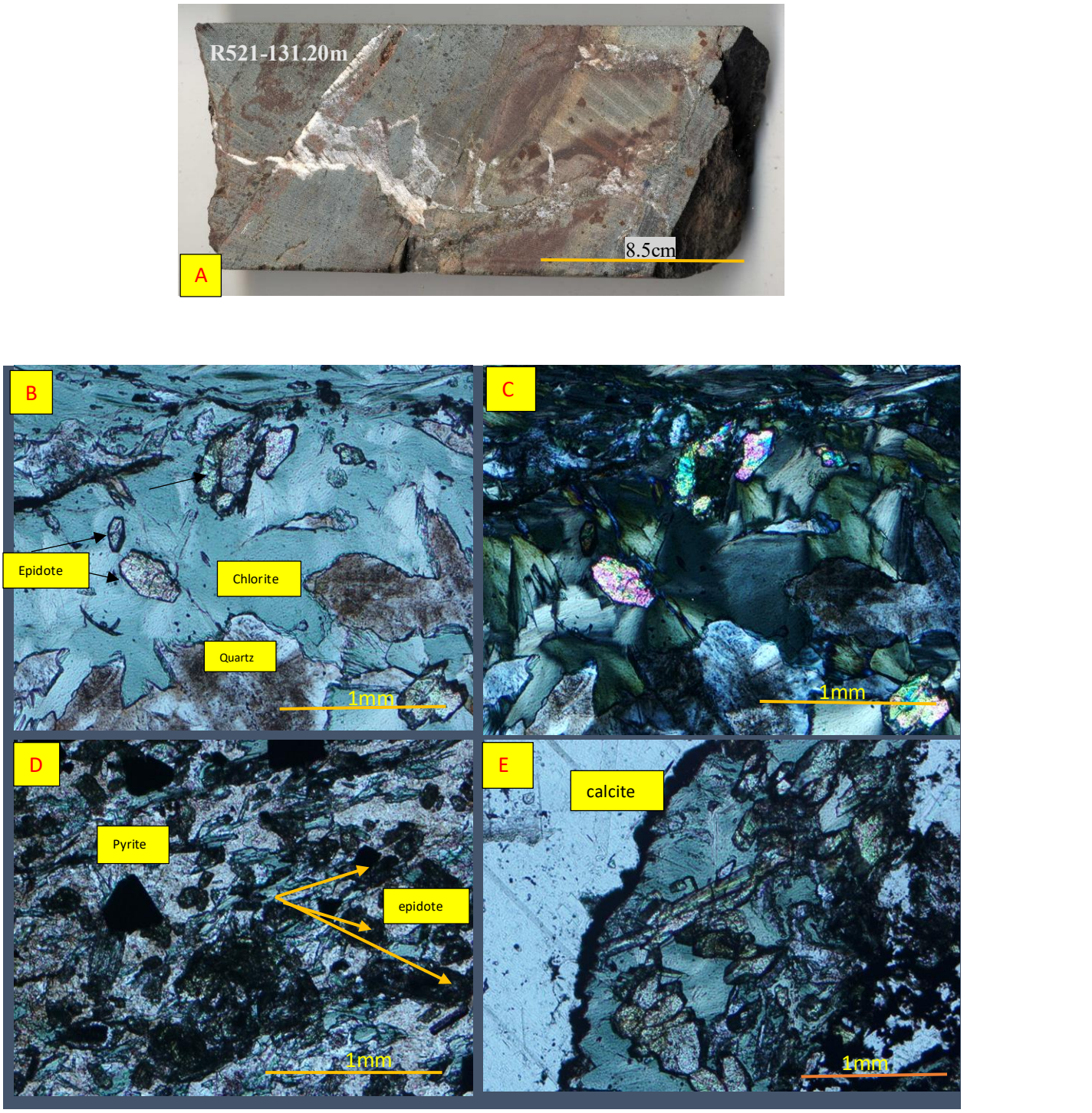

Figure 8. A) Drill core sample R521-131.30m, showing altered, mainly oxidized, and chloritized rock**.** Photomicrographs showing abundant chloritization, **B)** quartz mostly altered by chlorite and pseudo-hexagonal epidote, PPL. **C)** same in XPL. **D)** Pyrite grains with epidote. **E)** Chlorite, epidote, and Calcite with argillaceous filling between grains.

6.1.3 Dolomite

Dolomite samples are reddish-pinkish in color, recrystallized coarse grained with visible calcite veins and stylolite. Calcite consist of coarse grained pseudoform crystals probably formed by replacement of originally evaporites (Fig. 9a).

Petrographic study of representative dolomite samples includes micritic dolomite, some quartz, muscovite, and phlogopite. Dolomite here is replacement dolomite where it seems to be replacing original calcite crystal while original cleavage planes or fabric of calcite is retained (Fig. 9b-d). These are often called as saddle or pearlspar dolomite, showing coarse grains with undulose extinction having xenotopic fabric (Fig. 9c, f). Undulose extinction in dolomite grains without clear grain-grain contacts is an important indication of chemically formed dolomite that may be replacive of another mineral during burial. Moreover magnesium (Mg) is provided by conversion of smectite to illite during diagenesis where clay enriched rocks interbedded with carbonate strata, results in dolomitization (Győri et al., 2020). Though the little dedolomitization in which calcite replaces dolomite is also evident where rhombohedral dolomite crystal showing replacement fabric (Fig. 9g). Quartz occurs in minor amount as later vein filling (Fig. 9e). Phlogopite and muscovite shows typical sheet and fibrous appearance (Fig. 9c, f). Stylolites are present in dolomite which is an irregular surface in a rock formed by pressure solution. Usually stylolites have characteristic saw-tooth morphology and are associated with the accumulation of insoluble materials such as organics or iron oxides.

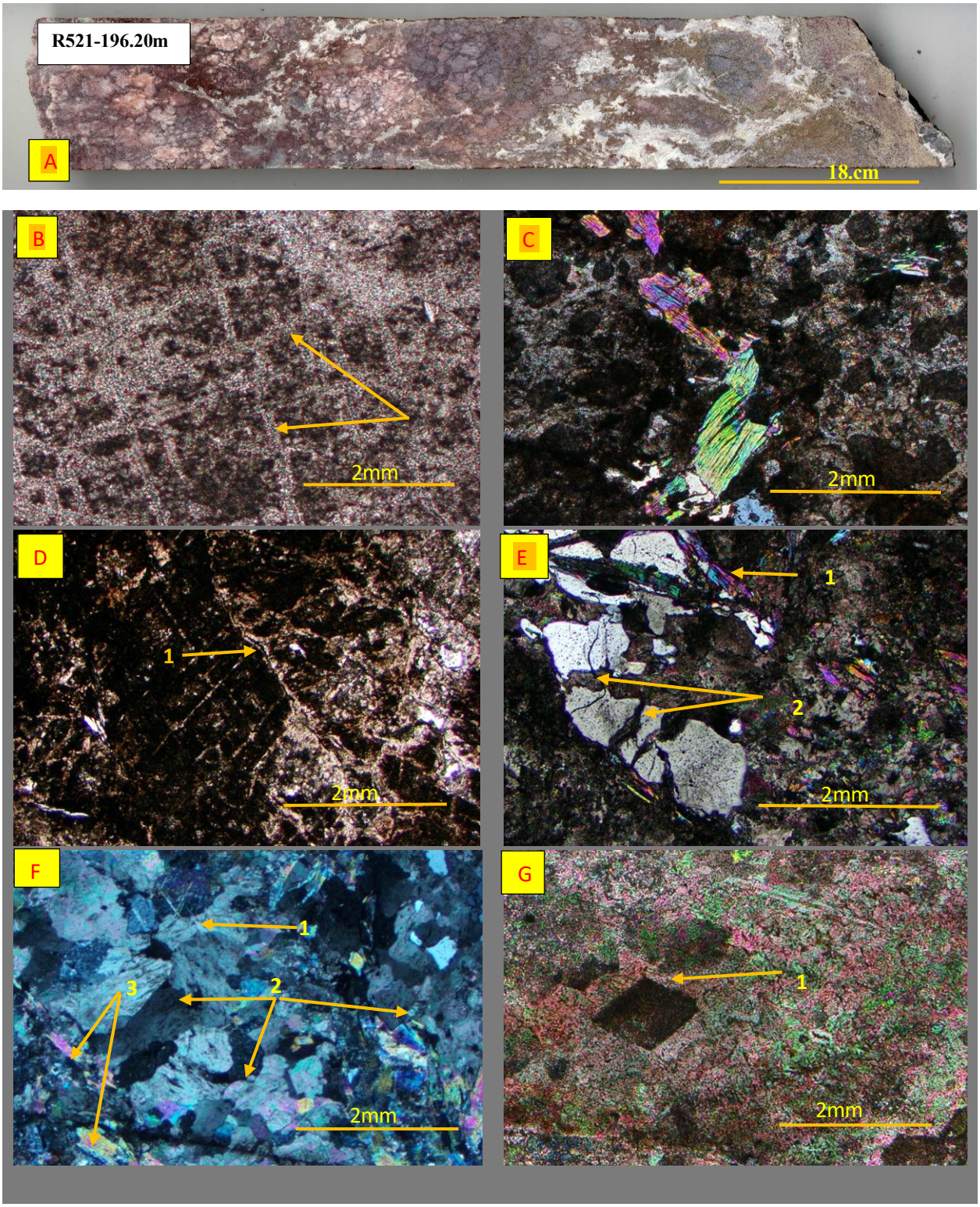

Figure 9. A) Scanned drill core sample R521-196.20m, vein filled dolomite. **B)** visible calcite cleavage planes, now dolomitized, PPL. **C)** Phlogopite grains, with xenotopic dolomite texture, XPL.**D)** stylolite and calcite vein filling, XPL**. E)** fractured quartz filling with muscovite 1 and calcite 2 grains. **F)** Undulose dolomite 2 and 1 coarse-grained calcite and fibrous muscovite 3, XPL **G)** A dolomite rhomb in a micrite, indication of dedolomitization, PPL.

6.1.4 Conglomerate

Sample of these breccia conglomerate from R105 are composed up of pinkish mudstone clasts which are rounded to subrounded with fine quartz and feldspar matrix (Fig. 10a). The fine/smooth touch suggest the presence of talc. Kyläkoski et al. (2012) describes these from the Petäjäskoski water channel as collapsed breccias up to tens of meters in thickness, clasts comprising from surrounding mudstones while evaporite layers dissolves during diagenesis, magmatic and hydrothermal processes.

Major composition of these conglomerates are clasts of mudstone and siltstone, quartz, feldspar, talc, micas, argillaceous matter, and opaque minerals. Quartz is present in smaller abundances than feldspars, usually rounded-subangular monocrystalline grains (Fig. 10c). Quartz overgrowth cement is commonly observed. The clasts of varied sizes are present ranging from coarse sand to granule size, usually of mudstone and siltstone with angular-subangular grain boundaries (Fig. 10b, g). The matrix content is greater than clasts making them para-conglomerates and of one clasts type as monomictic conglomerates or breccias. Feldspar includes plagioclase, orthoclase, and microcline with typical simple, polysynthetic and tartan/gridlike twinned grains (Fig. 10c, d, f). These are altered to kaolin and sericite with overgrowth feldspar cement, the concentration of feldspar is greater than quartz and exist as subrounded-rounded medium grains with epidote and rutile inclusions (Fig. 10f). These framework grains are placed in fine grained micaceous and argillic matrix. The fine matrix is sericite, and argillites like illite, chlorite, and kaolinite. Talc is present around 10-15 percent of whole rock and is composed up of laths and fan like texture (Fig. 10b). These are distorted around other minerals, sometimes breaking other mineral grains.

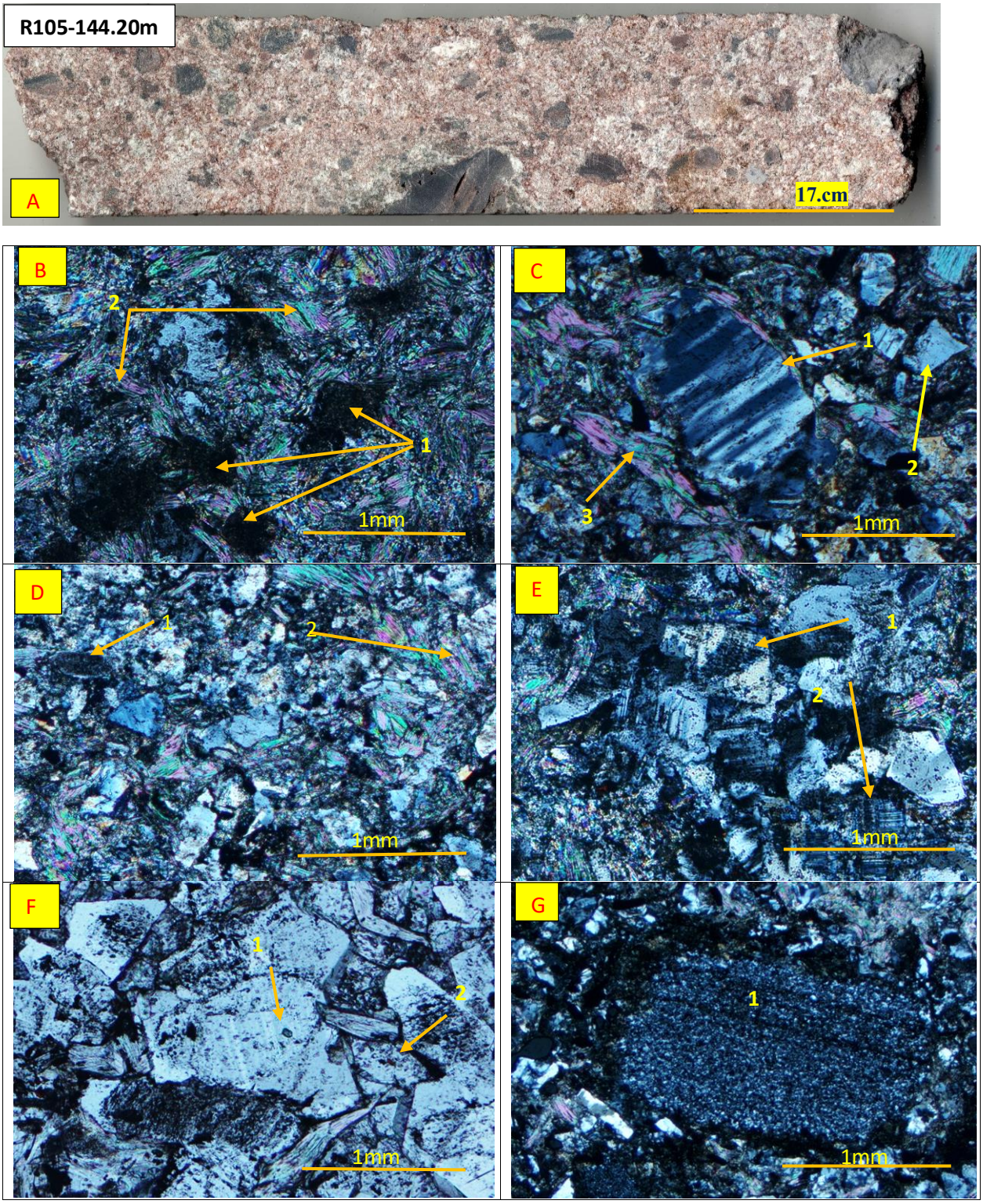

Figure 10. A) Scanned breccia sample of varying clasts**. B)** 1 is mudstone clast and 2 is talc in sericitic matrix, XPL. **C)** 1 is plagioclase, 2 is quartz and 3 is talc, dark is argillaceous matter, XPL **D)** 1 is orthoclase, 2 is talc, other grains are quartz and sericite matrix, XPL **E)** feldspar grains microcline 2 and plagioclase 1, feldspar overgrowth cement, XPL **F)** inclusions in feldspar 1 is epidote and 2 rutile, visible feldspar's alteration, PPL **G)** mudstone clast, contact been filled by argillaceous matter.

6.1.5 Recrystallized carbonate bearing sandstone

These are from 191m, 215m, and 193m locations. The sample 193m contains calcite pseudomorphs which are originally anhydrite and replaced afterwards by calcite during diagenesis (Fig. 12a).

The mineralogy of these samples includes quartz, feldspar, chlorite, biotite, muscovite, calcite while accessory minerals are zircon, rutile, hematite, and some opaque minerals. Quartz is major mineral about 50%-60% present both as monocrystalline and polycrystalline grains, which are sub-rounded to angular with interlocking fabric. Both undulose and simple extinction is present in quartz and is recrystallized quartz where deformation results in grain growth, sub grains rotation and protruding of grain boundaries at grain level producing intermingled quartz grains (Fig. 11b, f, g; Fig. 12f-g; Fig. 13b, e). Felspars include alkali feldspar (Orthoclase) and plagioclase (Albite), which both are clearly altered to sericite, having subrounded grains and make up about 15% of total rock (Fig. 11c; Fig. 12d-f; Fig. 13f-g). Plagioclase with both simple and polysynthetic twinning is evident. Chlorite is present in ample amount as 10-25% in these samples usually as laths distorted or oriented around other minerals grains and sometime present in vein like fashion, where complete layer of chlorite is present possibly because of chloritization across a complete horizon (Fig. 11f-g; Fig 12c, f). Micas are biotite and muscovite with typical sheet like and needle like grains and as inclusions in feldspar constituting about 10% of whole rock composition (Fig. 12c). Calcite is also abundant component of these samples occurring as medium-coarse closely packed grains (Fig. 11d-e; Fig, 12b, e, f; Fig. 13d). Trace amount of rutile, zircon, and iron oxide coating around some minerals and opaque minerals are present across the slide showing their detrital origin (Fig. 12d, g; Fig. 13e).

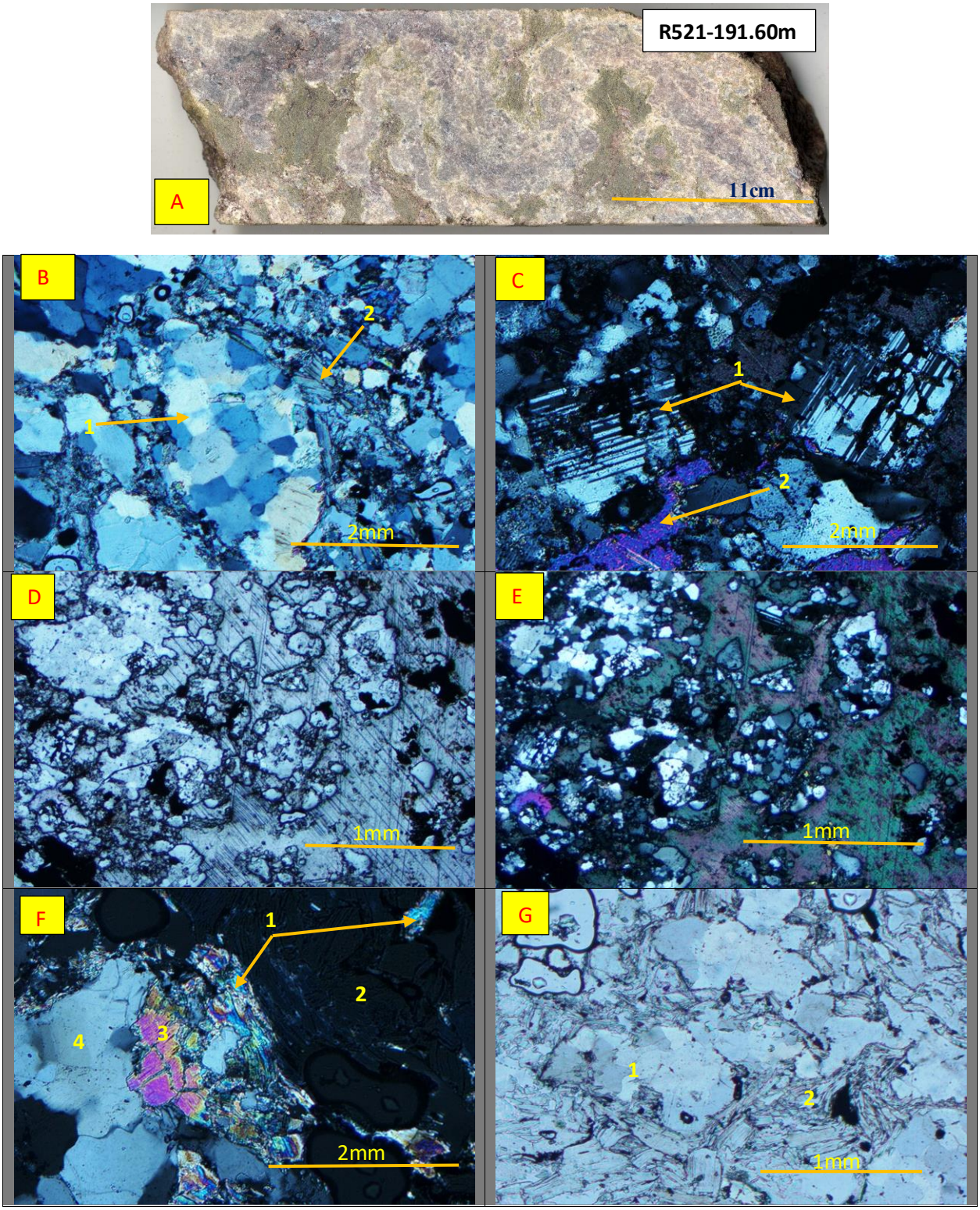

Figure 11. **A)** Scanned sandstone, patches of chloritization**. B)** 1 is recrystallized quartz, 2 is long chlorite grains. **C)** 1 is plagioclase, altered to sericite, 2 is calcite grains. **D)** recrystallized quartz in calcite, PPL **E)** same in XPL **F)** 1 is muscovite, 2 is chlorite, 3 is calcite and 4 is quartz, XPL **G)** same recrystallized quartz 1 and chlorite 2, PPL.

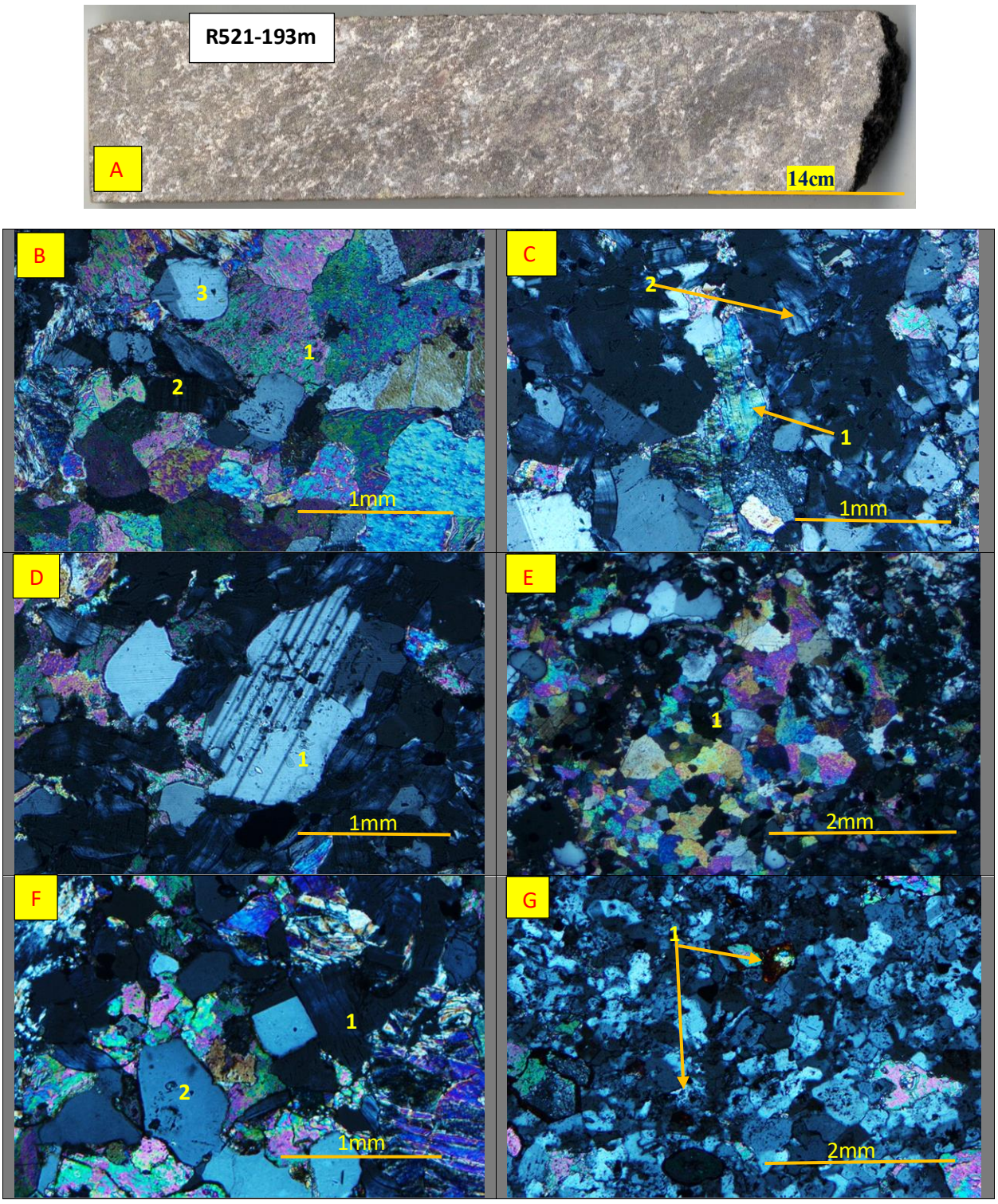

Figure 12. **A)** Coarse grained sandstone drill core sample. **B)** 1 is calcite, 2 is chlorite, 3 is plagioclase, XPL **C)** 1 is muscovite, 2 is chlorite, XPL **D)** plagioclase, with biotite and zircon inclusions, altered to sericite, surrounding grains are chlorite, calcite, and muscovite, XPL. **E)** 1 shows coarse grained calcite pseudomorph after anhydrite/gypsum enclosed by quartz and chlorite, XPL **F)** 1 is chlorite, 2 is monocrystalline quartz and in between them is calcite and plagioclase with simple twinning, XPL **G)** 1 shows rutile, quartz, and chlorite in surroundings.

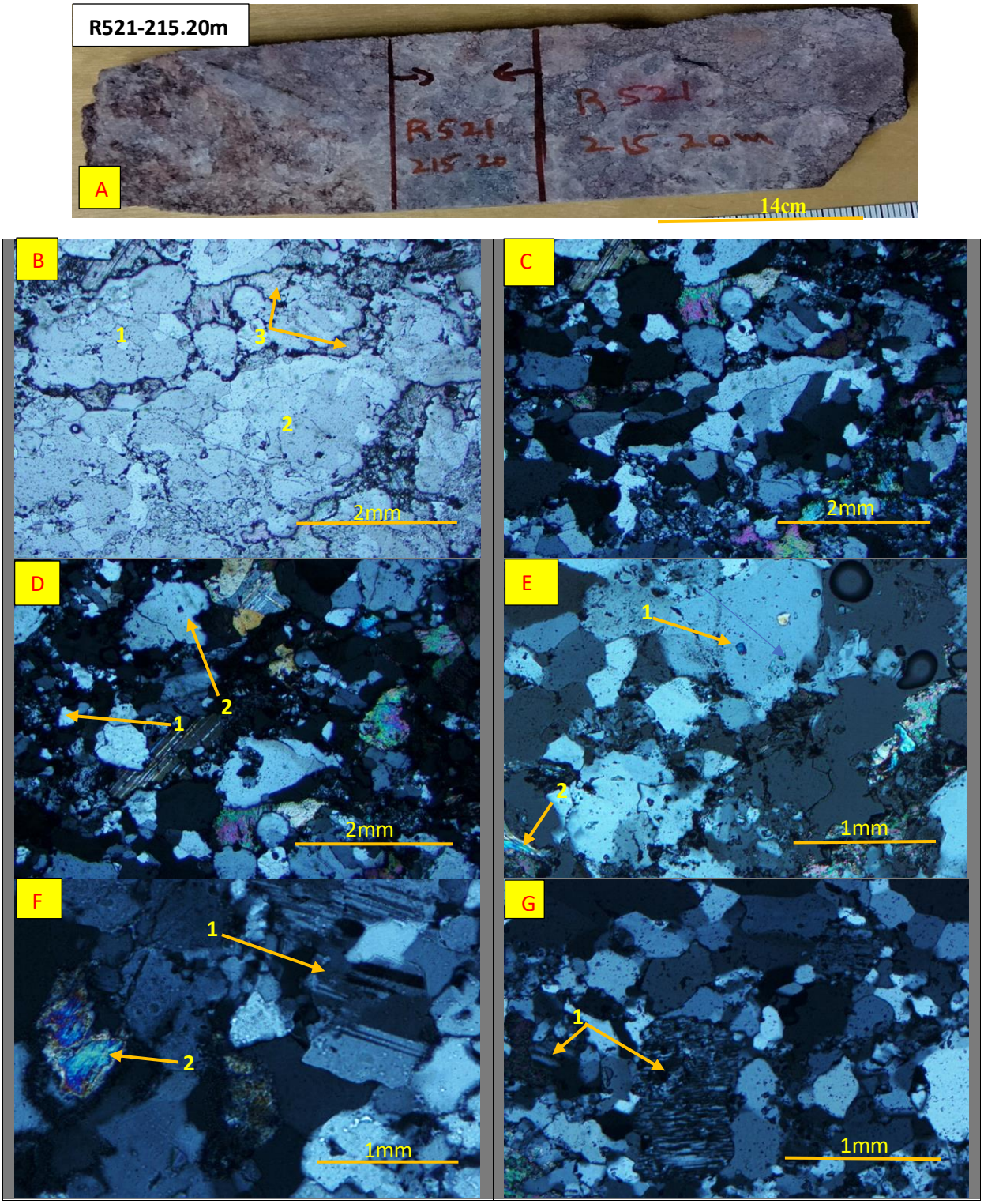

Figure 13. **A)** Scanned coarse grained sandstone sample. **B)** 1 and 2 is recrystallized quartz, sutured and interlocking contacts are evident, 3 is calcite filling spaces between grains, PPL **C)** same in XPL. **D)** 1 is fine grained angular quartz, 2 is quartz with zircon inclusion, bright color grains are calcite. **E)** 1 is zircon inclusion in quartz, 2 is muscovite. **F)** 1 is plagioclase with polysynthetic twinning, 2 is muscovite. **G)** 1 is orthoclase with patchy perthitic texture.

6.1.5 Sericitized sandstones

These includes the samples 233.46m, 234.70m, 221.50m, R521-240.47m, 241.55m. These samples have calcite rich voids/cavity fillings as replacement whereby older evaporitic intercalations were possibly dissolved/leached and replace by calcite (Fig. 14a-b; 15a; 16b, c; 17a, c; 18a, c).

Petrographic studies shows that these drill samples are deeply altered with abundant vein fillings. Overall rock composition is quartz, feldspar, muscovite, calcite, sericite, titanite and argillaceous matter. Quartz present here is fine to medium grained, with undulose extinction monocrystalline with few polycrystalline grains. These are rounded to subangular fractured grains making up 30% of whole rock (Fig. 14e; 15d; 16e). Feldspars are orthoclase and plagioclase with simple and multiple twinning grains. These feldspar are rounded to sub angular making up the 25% of rock (Fig. 14e; 15c; 16d-e). Feldspar is fractured and severely altered to sericite and kaolin referring to their cloudy and patchy appearance. Feldspar also has overgrowths as authigenic feldspar formed on both plagioclase and potash feldspar grains during diagenesis, where sodium is being provided from dissolution of smectite to illite. Both quartz and feldspar occur as coarse grains in a fine-grained carbonate and sericitic matrix and visually seems like floating in matrix. Overall, these samples are poorly sorted. Calcite is present in abundance in these samples ranging from 10%-15% of whole rock (Fig 14b, c; 15b; 16b-c). Quartz grains are broken because of calcite precipitation in fractures of grains. Muscovite is present in vast amount (15%) with typical laths oriented around quartz and feldspar grains, altered extensively to fine grained sericite (Fig. 14d; 15c, e; 16d-e). Rutile is present in trace concentrations (Fig. 14e). Carbonaceous matter also exists in ample percentages around 10% of overall rock composition often cutting the other mineral grains suggesting their secondary origin (Fig 14c, d). Zircon, rutile, and epidote as inclusion is found in these samples (Fig. 17b; 18b). Iron oxide possibly hematite as fine disseminated grains along with some opaque minerals are present in trace amount. Cementing material for these rocks are kaolinite, sericite, quartz overgrowth, and calcite (Fig. 18b-c).

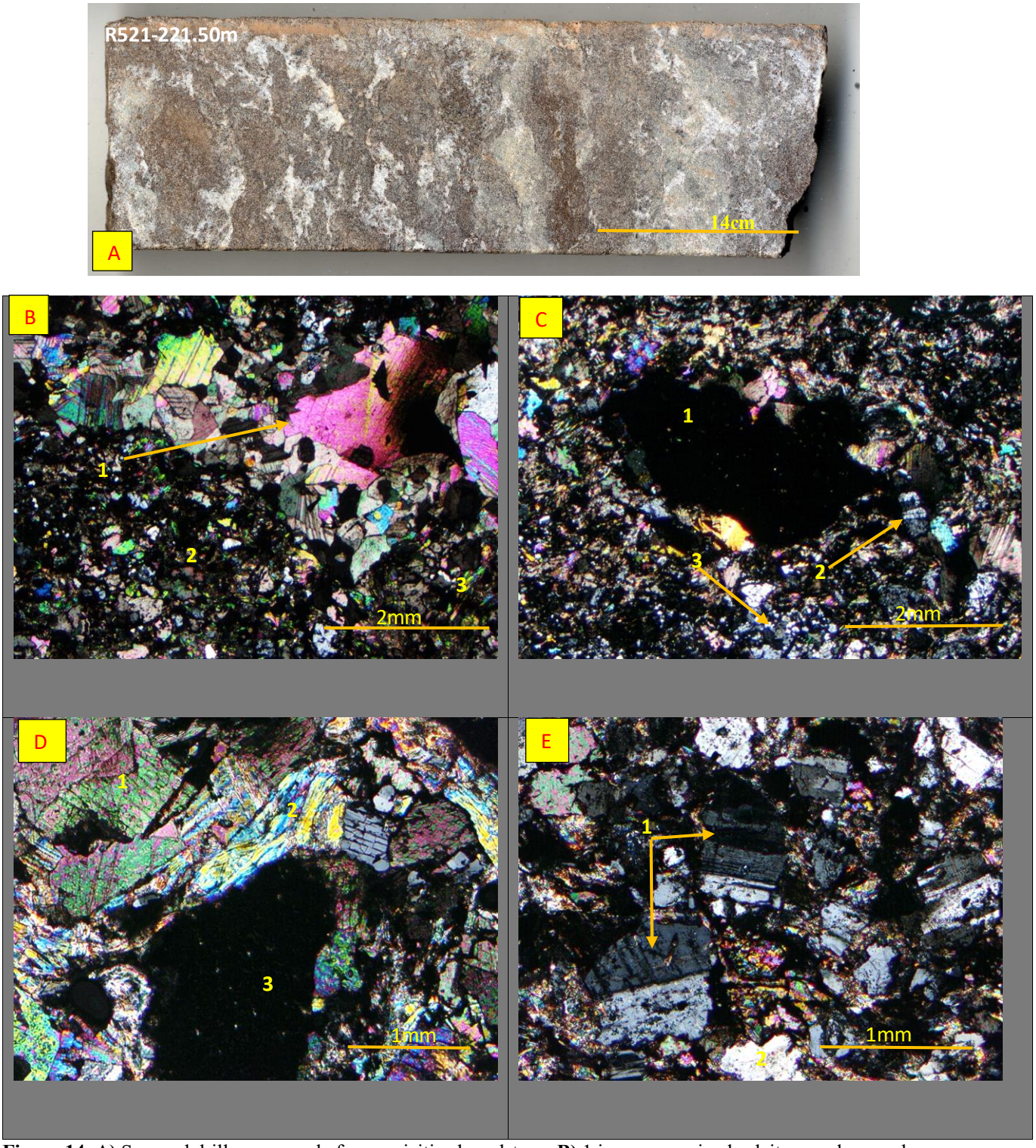

Figure 14. A) Scanned drill core sample from sericitized sandstone. **B)** 1 is coarse grained calcite pseudo-morph after anhydrite/gypsum, 2 is quartz, feldspar in fine matrix, dark grains are argillaceous matter, 3 is muscovite, XPL **C)** 1 is organic matter, 2 is plagioclase and 3 is fine grained quartz, XPL **D)** 1 is calcite, 2 is muscovite and 3 is organic matter, XPL **E)** 1 is close view of plagioclase with visible alteration, twins, and rutile inclusion, 2 is quartz bright grains are calcite.

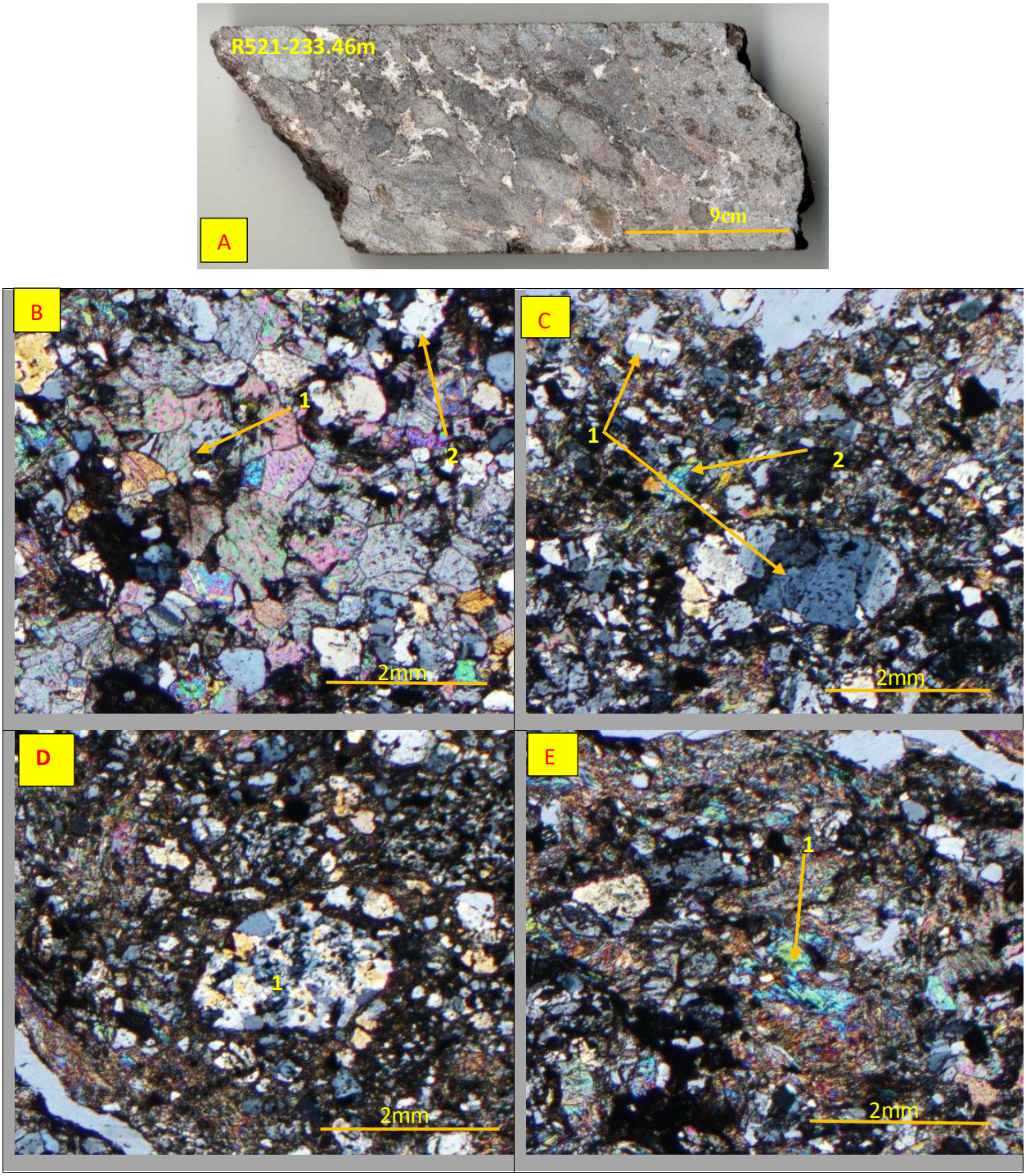

Figure 15. A) Scanned lithic sandstone drill core sample. **B)** 1 is calcite, 2 is plagioclase, XPL **C)** 1 is plagioclase, 2 is muscovite, XPL **D)** 1 sandstone clast, multiple quartz grains in a fine sericite, XPL **E)** 1 is muscovite, other are angular quartz and feldspar, XPL.

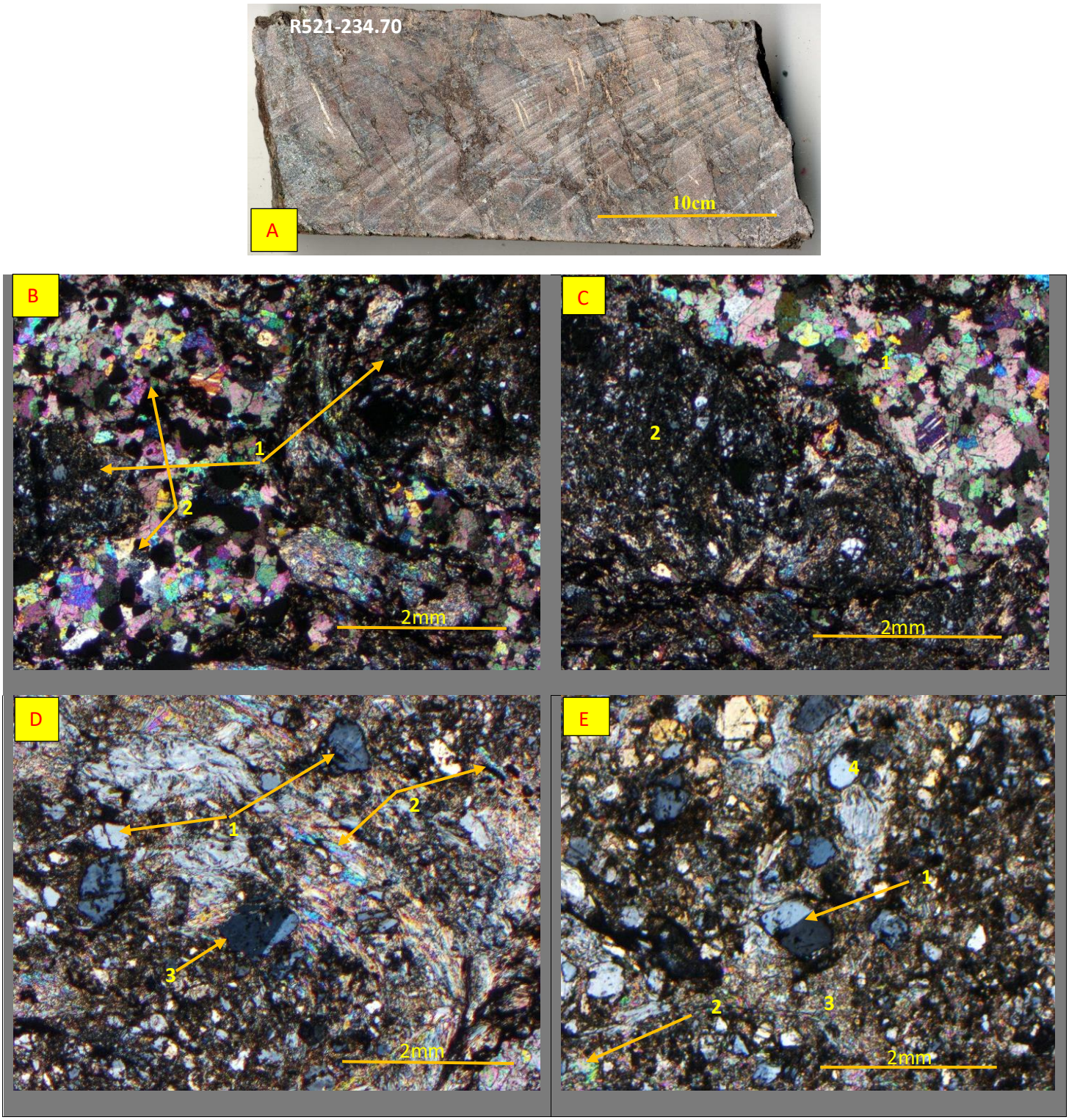

Figure 16. A) Scanned drill core patchy sandstone. **B)**1 is fine grained quartz and feldspar in sericite matrix, 2 is coarse grained calcite pseudomorph after anhydrite/gypsum, XPL **C)** 1 is fine grained quartz and 2 is calcite pseudomorph after anhydrite/gypsum, XPL **D)** 1 is orthoclase, 2 is distorted muscovite, curved shape due to stress and 3 is plagioclase, XPL **E)** 1 is plagioclase, 2 is muscovite, 3 is fine sericite 4 is quartz, XPL.

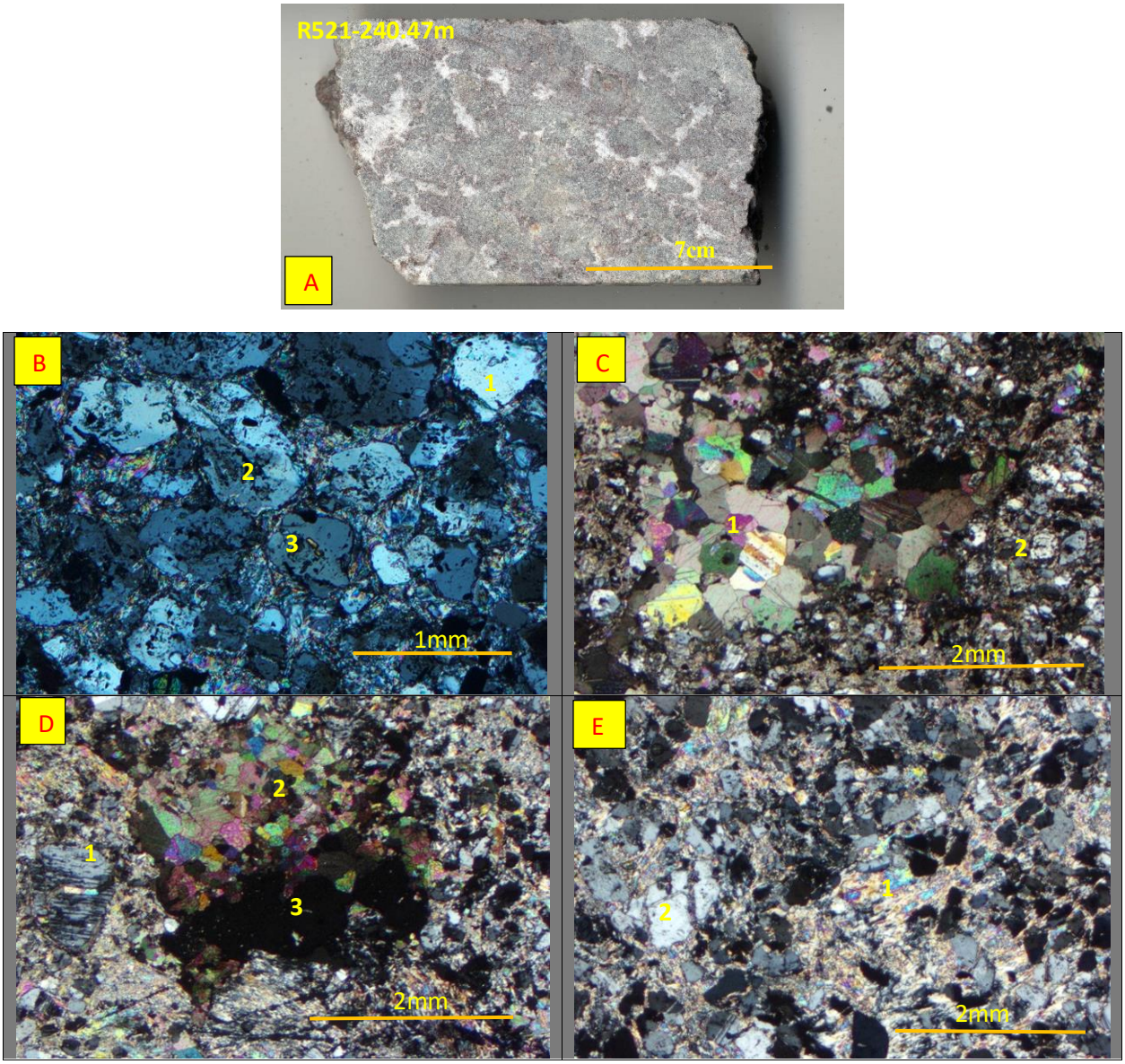

Figure 17. A) Scanned drill core sandstone sample. **B)**1 is quartz with zircon inclusions, 2 is orthoclase with epidote and 3 is orthoclase with rutile inclusions in a sericite matrix, XPL **C)** 1 is coarse calcite pseudomorph after anhydrite/gypsum .and 2 is quartz and feldspar in fine matrix poikilotopic texture, XPL **D)** 1 is plagioclase with biotite inclusion and 3 is organic matter, XPL **E)** 1 is muscovite and sericite while 2 is orthoclase grain fractured by sericite, XPL.

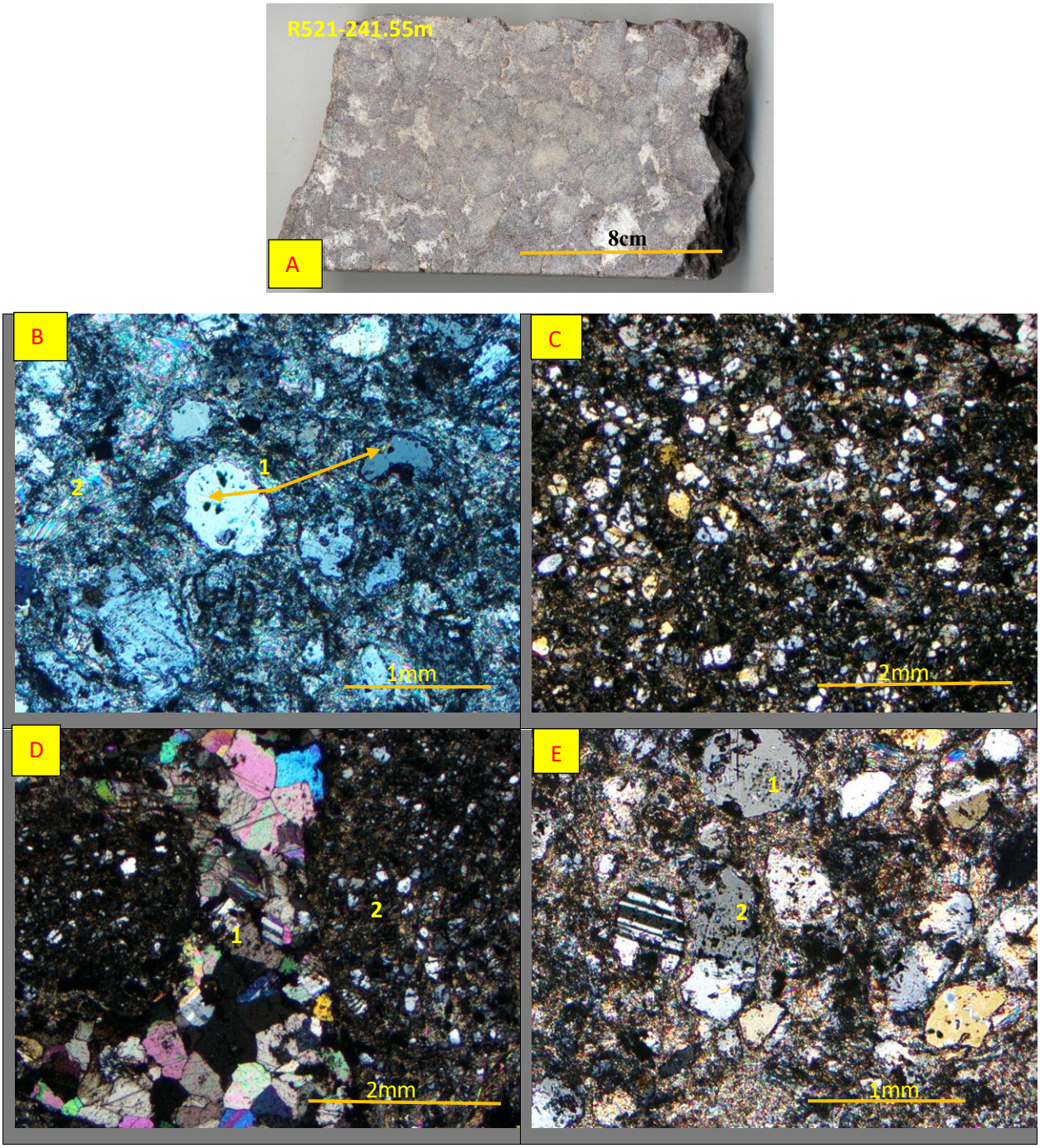

Figure 18. A) Scanned drill core sandstone sample. **B)** 1 is quartz grain with zircon and rutile inclusions, XPL **C)** medium grained quartz, plagioclase, and orthoclase in a fine sericite matrix (poikilotopic texture) XPL. **D)** 1 is coarse grained calcite pseudomorph after anhydrite/gypsum and 2 is quartz and feldspar in matrix, XPL **E)** 1 is quartz with abundant inclusions, 2 is plagioclase with polysynthetic twins, in a matrix of fine-grained muscovite.

6.1.6 Sub-arkose sandstone

These includes sample from 241.60m, 244m and 261.97m locations (Fig.19a; 20a; 21a). Petrography examinations of sandstone samples shows varied concentrations of framework grains mainly quartz and feldspars. The accessory matrix includes biotite, sericite, chlorite, muscovite, and hematite in varied proportions. Overall texture of these drill core samples ranges from medium to coarse grained with well sorted and subrounded- rounded mineral grains showing textural maturity. These grains are bounded together by clay minerals, siliceous (quartz overgrowth) and calcareous cement. The contact between grains ranges from concave-convex, sutured, and long boundaries. Quartz makes the most abundant of framework grains after feldspar constitute about 65% to 70% of total rock composition. The quartz grains are unaltered subrounded-rounded, moderately sorted with long and sutured fabric. Majority of them are monocrystalline (Q_m) while only some grains are polycrystalline (Q_p) (Fig. 19b- d; 20c, d, g; 21c, e). Undulatory/ wave/strained extinction with varied extinction angles are present in quartz grain both in monocrystalline and polycrystalline grains illustrating partial retrieval of grains after a deformation event. Some polycrystalline grains have more than three grains while single clear quartz unit is abundant. Though most grains are unaltered, but some are fractured and cloudy unlike common quartz grains. Inclusions include biotite and zircon placed sporadically within quartz crystals. Feldspar of various compositions, grain sizes and shapes form the second largest constituents of these quartzite samples averaging about 25%. Among feldspar microcline and orthoclase (Alkali feldspar) are in ample amount ranging from 25-32% compared to albite and anorthite (Plagioclase feldspar) having average concentration of about 10%. Grains are subrounded-rounded, occasionally with irregular boundaries having diffuse contacts with surrounding grains. 65%-75% of feldspar grains seems cloudy/turbid in thin section suggesting abundant kaolinitization with formation of illite, sericite. Microcline is present in abundance and clearly shows crosshatch/gridlike/tartan twinning pattern forming grid pattern on (100) plane (Fig. 19b, e- g; 20c- e; 21d-e). Alteration of microcline to sericite and ilmenite is common and clearly visible. Orthoclase lacks twining but perthitic texture and typical cloudy appearance due to scattered kaolin and alteration is evident. Plagioclase feldspar is least in concentrations in these samples and shows diagnostic polysynthetic twinning along with alteration. Accessory minerals include biotite, muscovite, chlorite, hematite, opaque mineral, calcite, and zircon and are present in minor or trace proportions. Also, zircon and biotite are found as inclusions within quartz grains. Micas like biotite and muscovite shows typical sheet like

medium grained laths bent or twisted showing compaction accounting for 8-10 percent of whole rock forming also part of the matrix of the sandstones (Fig. 19c, e- g; 20f-g; 21d). Heavy minerals like zircon and epidote shows trace presence (Fig. 19b; 20g). Chlorite is found as fine-grained cement filling and as well-developed grains (Fig. 20f). Calcite is present as cementitious material between the grains (Fig 19b, d).

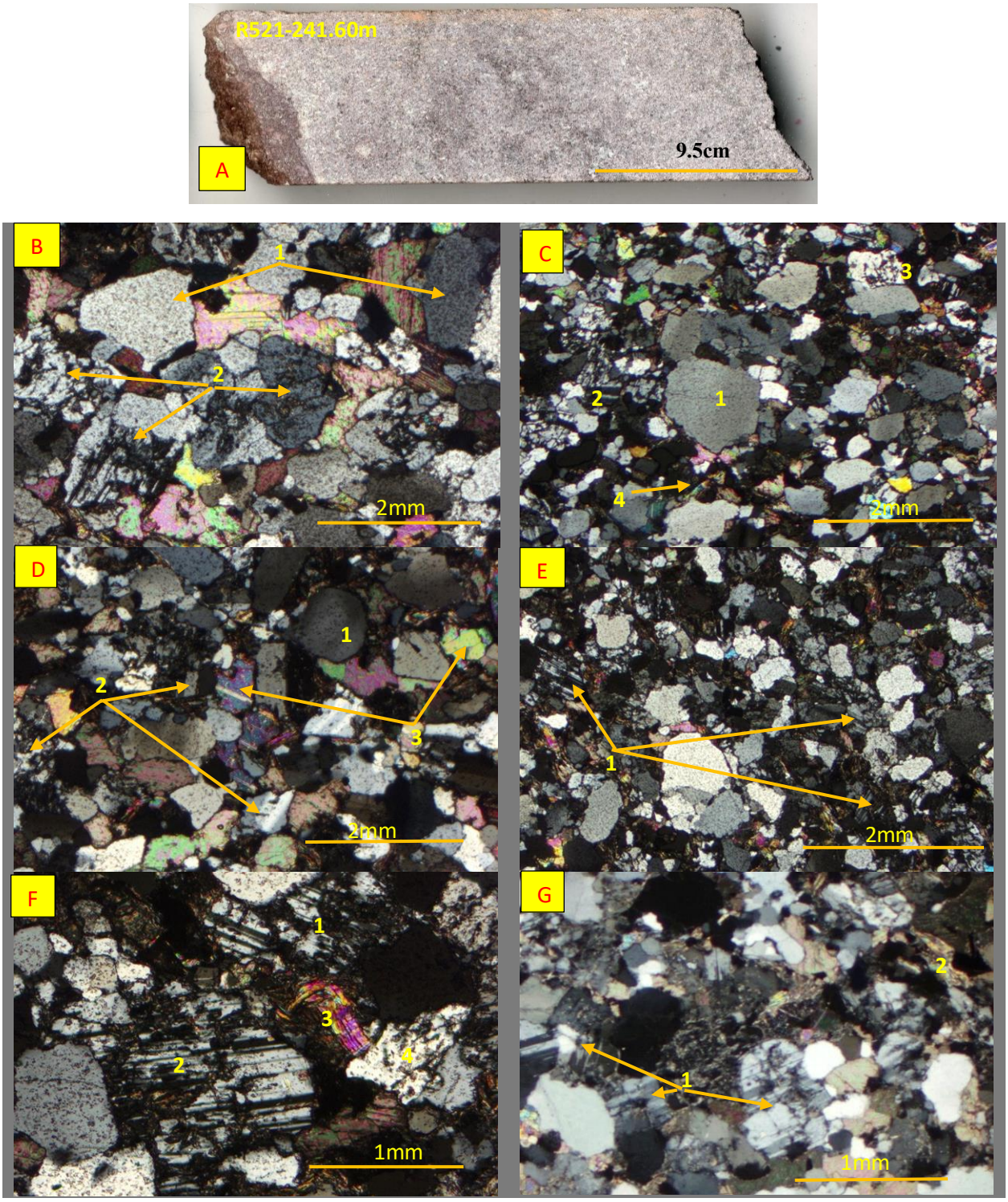

Figure 19. A) Scanned drill core coarse grained sandstone. **B)** 1 I monocrystalline subrounded quartz with inclusions, 2 is orthoclase with sericitic alteration, bright grains are calcite, XPL **C)** 1 is quartz, 2 is plagioclase, 3 is orthoclase and 4 is muscovite, XPL **D)** 1 is well rounded quartz, 2 is plagioclase and 3 is calcite, XPL **E)** 1 is plagioclase, 2 is muscovite, other grains are quartz and calcite XPL. **F)** 1, 2 is plagioclase, sericitized and biotite inclusions, 3 is muscovite and 4 is orthoclase, XPL **G)** 1 is altered plagioclase and 2 is biotite, XPL.

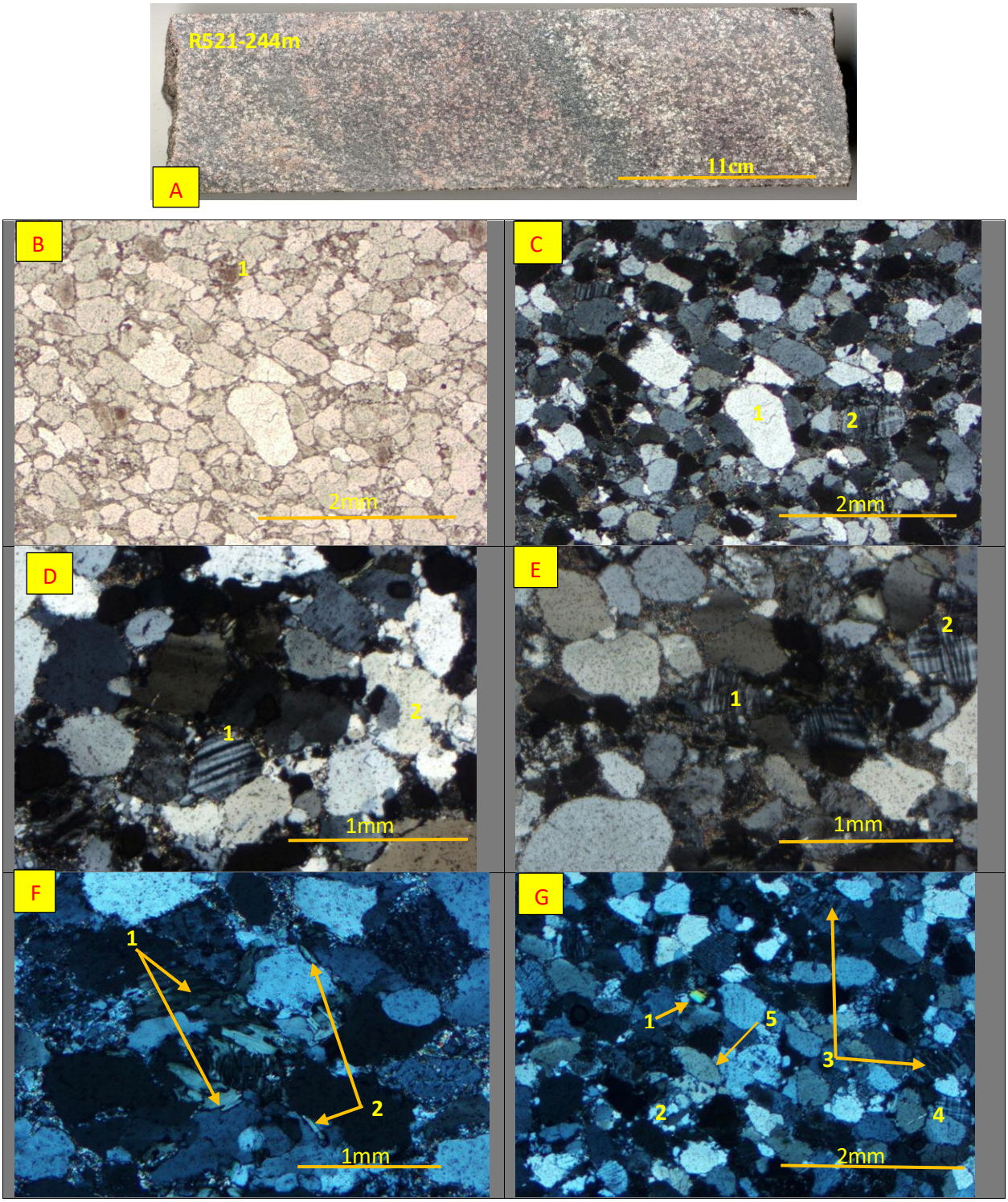

Figure 20. A) Scanned drill core coarse grained sandstone. **B)** 1 is orthoclase with patchy appearance, other quartz and feldspar bounded by fine grained muscovite, PPL **C**) 1 is quartz with long and sutured contacts, 2 is plagioclase, XPL **D)** 1 is plagioclase and 2 is polycrystalline quartz, XPL **E)** 1 is plagioclase and 2 is microcline, other grains are quartz and muscovite matrix, XPL **F)** 1 is chlorite and 2 is biotite, both sides of 2 is visible feldspar alteration, XPL **G)** 1 is biotite, 2 is polycrystalline quartz, 3 is plagioclase, 4 is microcline and 5 is quartz with zircon inclusions, XP

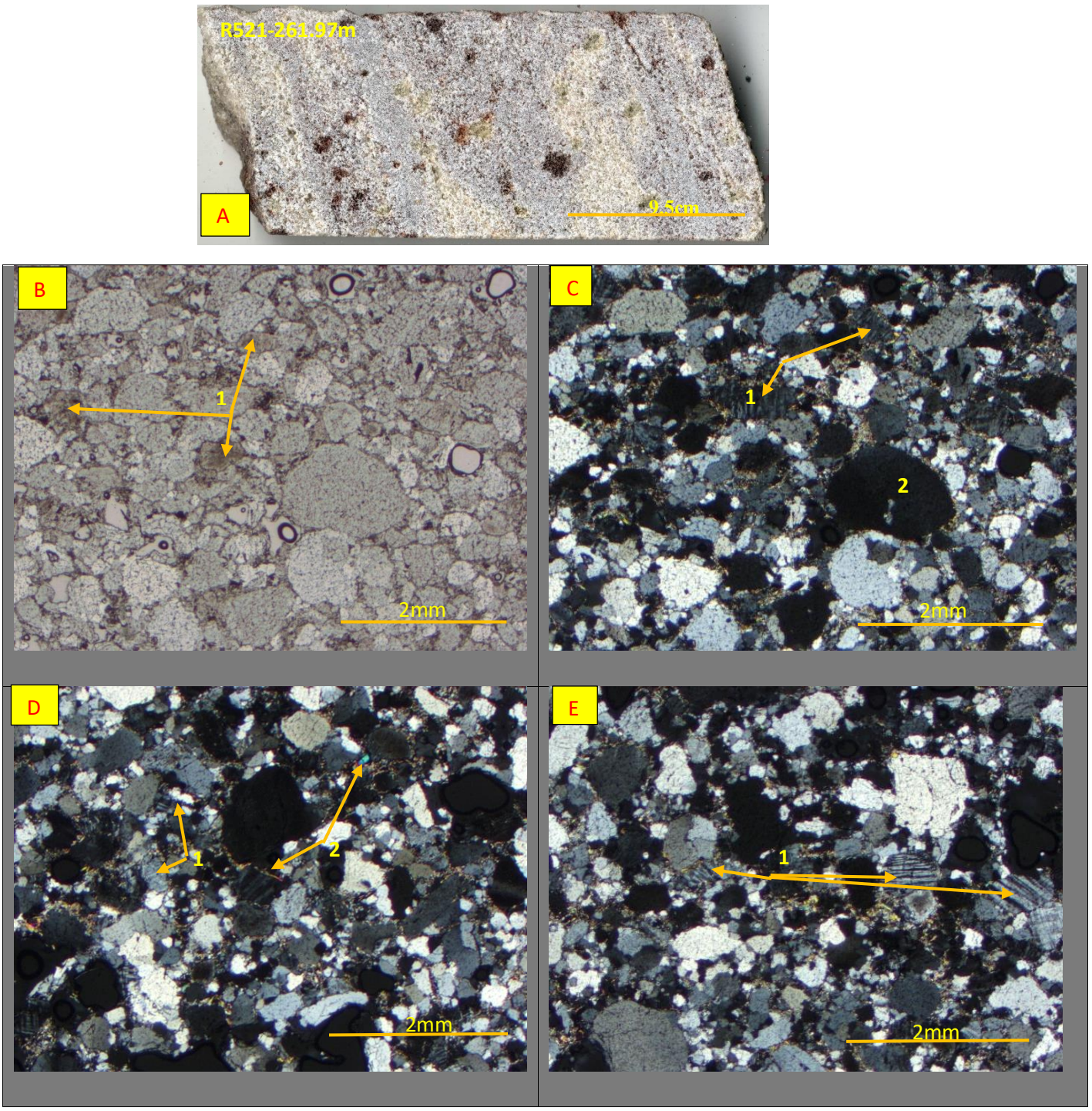

Figure 21. A) Scanned coarse grained sandstone visible layering. **B)** 1 is orthoclase in coarse-grained, well-rounded quartz and feldspar, PPL **C)** same in XPL, 1 is plagioclase and 2 is quartz, bounded by fine grained muscovite **D)** 1 is microcline and 2 is biotite, XPL. **E)** 1 is plagioclase, other grains are quartz and fine muscovite, XPL.

6.2 Electron Microprobe Analysis

The electron microprobe analysis of six carbon coated thin section samples of the Petäjäskoski formation were performed (Table 3). The aim is to identify and determine the chemical compositions of possible evaporitic minerals, especially anhydrite and halite. For the microprobe analysis a current beam of 10nA because at higher beam evaporites if present may be dissolved, and voltage of 15kV is being used. The results show only trace amount of anhydrite in R521-193.40m (Table 4, 5; Fig. 22), minor halite in R521-193.40m as suggested by grain morphology although EDS is not confirming the composition of halite (Table 6; Fig. 23), and some bischofite and sylvite in R521-215.20m sandstone sample (Table 7; Fig. 24) of Petäjäskoski formation. These samples are located above and below dolomite unit. The Energy dispersive spectrometer (EDS) is commonly used for determining composition, only for one sample of anhydrite WDS is used because small crystals/grains of these salts will be destroyed by using Wavelength dispersive spectrometer (WDS).

Table 3. Showing thin sections analyzed in Electron Microprobe.

Thin section no	**Rock type**
193.40m	Recrystallized carbonate bearing sandstone
215.20m	Recrystallized carbonate bearing sandstone
221.50m	Sericitized sandstone
233.46m	Sericitized sandstone
240.47m	Sericitized sandstone
241.55m	Sericitized sandstone

Microprobe Results for R521-193.40m

Table 4. Showing Energy dispersive spectrometer (EDS) composition of anhydrite in a Feldspar, R521-193.40m.

	O	Na_2O	Al_2O_3	SiO_2	SO_3	CaO	Mineral
1	0				61.59	38.41	Anhydrite
2	0	11.84	20.51	67.65			Plagioclase

Table 5. Showing Wavelength dispersive spectrometer (WDS), results of anhydrite.

SiO_2	MgO	CaO	SO_3	Na_2O	Cl	Total
0	0	42.225	56.751	0.046	0.014	99.033

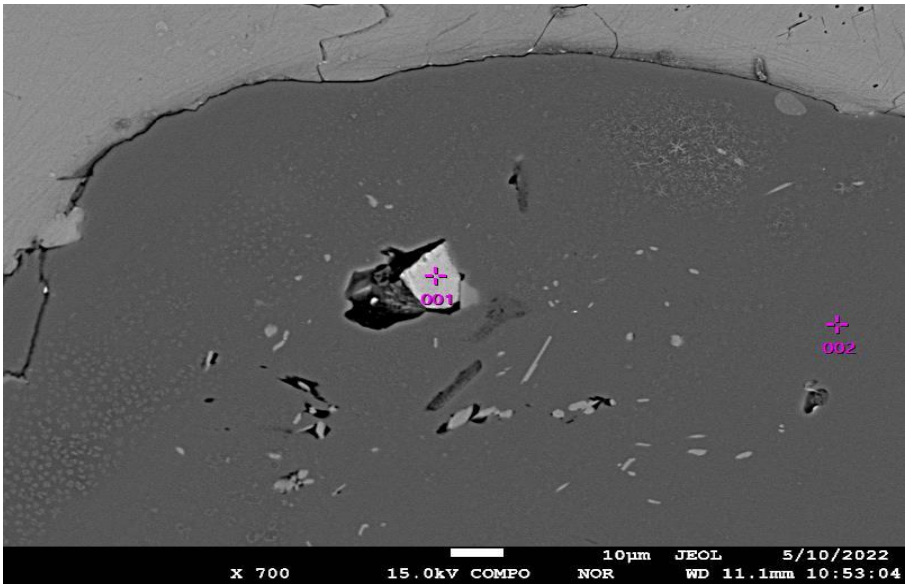

Figure 22. Back scattered electron (BSE) image of anhydrite inclusion in (Albite) Plagioclase Feldspar, R521-193.40m Sandstone of Petäjäskoski formation.

Table 6. Showing EDS composition of possible halite in a calcite, R521-193.40m.

	C	O	Na_2O	Al_2O_3	SiO_2	Cl	K_2O	CaO	Mineral
1	1.24	0	0.63	13.48	16.35	0.83	2.82	64.64	Halite
2	2.74	0						97.26	Calcite

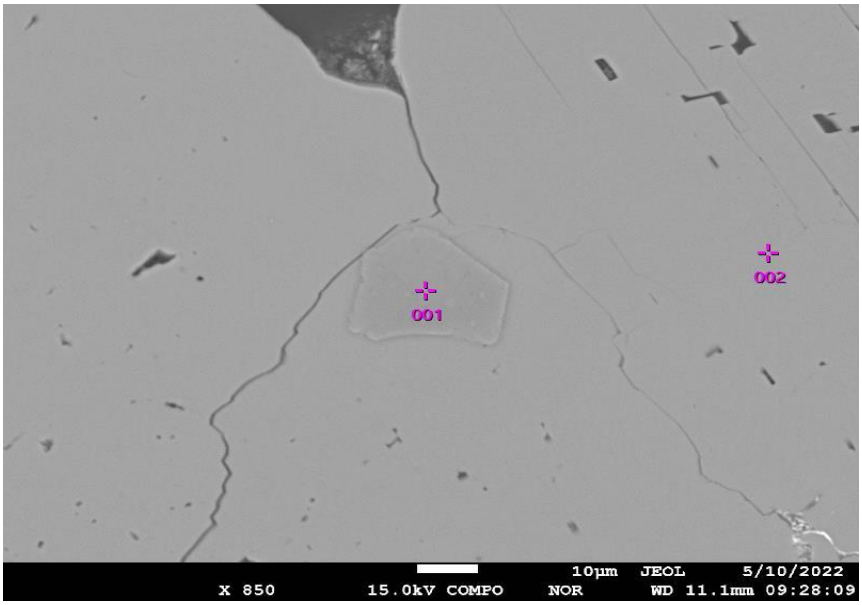

Figure 23. Back scattered electron (BSE) image of possible halite in calcite, R521-193.40m, Sandstone of Petäjäskoski formation

Microprobe Results for R52-215.20m

Table 7. Showing Energy dispersive spectrometer (EDS) composition of bischofite and sylvite in alkali Feldspar, R521-215.20m.

	O	Na_2O	MgO	Al_2O_3	SiO_2	Cl	K_2O	FeO	Mineral
1	0	0.98	18.86	8.69	37.7	14.22	19.54		Bischofite
2	0	1.25	2.52	1.36	64.31	14.2	16.36		Sylvite
3	0	0.96	10.36	5.31	57.49	10.97	14.91		Clay mineral
4	0	2.12	19.74	11.62	39.82	10.54	14.52	1.63	Alkali Feldspar

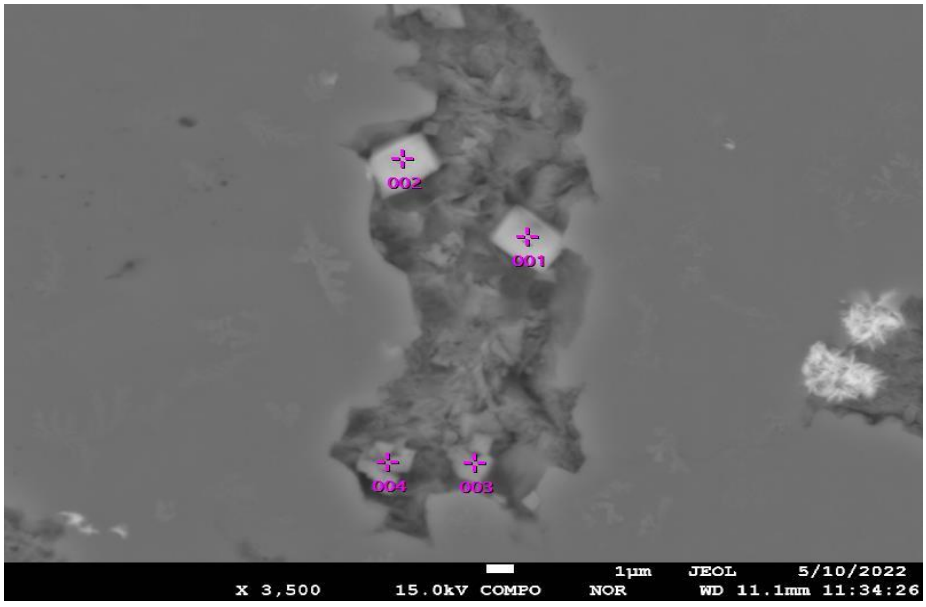

Figure 24. Back scattered electron (BSE) image of bischofite MgCl/sylvite (KCl) and some clays in alkali feldspar, surrounding material is quartz, R521-215.20m, Sandstone of Petäjäskoski formation.

7. Discussion

The objective of this thesis is to characterize the Petäjäskoski formation through petrography and microprobe (EMPA) in the Paleoproterozoic Peräpohja belt in three drill holes and to further substantiate the existence of evaporite occurrence within the Petäjäskoski formation as these are important in deciphering the genesis of different ore deposits in the Peräpohja belt, e.g. base metal rich orogenic deposits like Rompas-Rajapalot Au-Co (Ranta et al., 2018; Tapio et al., 2021) and stratiform deposits where evaporites provides chlorine for metals transport during hydrothermal processes (Saintilan et al., 2018).

Kyläkoski et al., (2012) described the collapsed monomictic breccias within the Petäjäskoski formation where clasts were from adjoining albite schist owing to dissolution of evaporitic unit. The result of this study shows trace amount of anhydrite, halite, sylvite and bischofite in sandstone units of Petäjäskoski formation which further supports the evaporitic origin of the PFm. Also, the presence of talc and phlogopite in mudstone samples supports the existence of Mg-bearing solutions originating from evaporites within Petäjäskoski formation (Yantambwe and Cailteux, 2019). Recently, several known potential evaporitic intersection have been found from the Central Lapland belt (Haverinen, 2020) and the Peräpohja belt (Tapio et al., 2021). Also well-known Paleoproterzoic evaporitic succession are described from Onega basin Russia (Melezhik et al., 2012) and Alta–Kvaenangen Tectonic Window, Norway (Melezhik et al., 2015).

In Russia, Onega basin >200m thick anhydrite and halite is encountered during drilling below the dolomite having ^{13}C isotopic values corresponding to marine carbonates deposited during Lomagundi-Jatuli event of 2.2-2.06 Ga where the ^{13}C values of PFm dolomite (Karhu, 1996) is in range of +5.2 to +10.6 referring to same phenomenon. The presence of these evaporites below the dolomites in Russian Onega suggests these basins were forming sulphate at same time with oxidized shallow marine and subaerial environments (Melezhik et al., 1990, 2015).

Extensive chloritization in supracrustal strata of Peräpohja belt is attributed to hydrothermal activity which dissolves and remobilize proposed evaporite sequence of the Petäjäskoski formation and produces Na, Cl rich fluids which are responsible for formation of atypical Au-Co-U occurrences of Rompas-Rajapalot in northern part of Peräpohja belt (Yardley and Cleverley, 2014; Melezhik et al., 2015; Ranta et al., 2018). Such albitization of Cambrian rocks were also reported from Norway, Sweden, Russia, and other northern parts of Finland and associated with Au-Cu and Fe deposits in Fennoscandia (Frietsch et al., 1997). Evaporites and collapsed breccias are found in the deep drill cores of the Matarakoski formation of Savukoski group in the Central Lapland belt (Haverinen, 2020), Moreover, a scapolite formation in Precambrian rocks of central Lapland belt CLB can also be explained by chlorine metasomatism where chlorine originated from these evaporitic rocks of CLB (Tuisku, 1986).The presence of phlogopite and sericite along with chlorite in mudstone and sandstone suggest these rocks have gone through lower greenschist facies metamorphism.

The presence of chlorite as neoformed intergranular cement and occurrence of halite in feldspars in sandstone during microprobe studies suggests that at least some of the albite and chlorite have syn-burial origin and predates the other events associated with known mineralisation at e.g., Rajapalot. This also means that these minerals may have been present at the time of later mineralisation events which indicates that they may simply be remobilised rather than reflecting the composition of mineralising fluid.

The Petäjäskoski formation is sandstone-mudstone-dolomite unit with some breccia sequence, altered/deformed in between competent rock of Palokivalo and Jouttiaapa formation. The sedimentary structure observed during drill core logging includes flaser and lenticular beddings, rhythmic dark and light intercalated laminations, drapes in claystone-siltstone collectively known as mudstone, layers in sandstone of PFm and collapsed breccia and brecciation within mudstone unit. The presence of micro-textures like calcite rosette, pseudomorphs after anhydrite/gypsum and calcite replacement in fractures which originally was occupied by evaporitic minerals and later replaced by calcite during diagenesis is another important indication of evaporitic conditions during the deposition of Petäjäskoski formation. Also, Desiccation cracks and stromatolites in dolomite has been reported by Kyläkoski et al., (2012). Additionally, the absence of preserved microbial structures suggests high clastic input or chemically precipitated material. Therefore, we suggest either lagoonal or shallow ramp tidal-flat evaporitic conditions where salt saturation limit was surpassed as suggested by sylvite in microprobe studies. The depositional setting was not exposed to contamination from open ocean water, where purely chemical co-precipitation of gypsum-dolomite and organics originating from other types of bacteria/algae occurred that are abundant enough in this environment to produce preserved organic matter (Adnan et al., 2015).

Distinctive features like collapsed breccia, pseudomorphs of anhydrite in Petäjäskoski formation, trace amount of halite, bischofite, sylvite, and anhydrite in microprobe studies, extensive albitization and presence of distinct evaporites in adjoining Central Lapland belt and thick anhydrite beds in northern part of Peräpohja belt evidently confirms the groundbreaking work of Kyläkoski et al. (2012) that these rocks were deposited in evaporitic conditions, thus making them the oldest known Paleoproterozoic occurrence of evaporites in Fennoscandian shield.

8. Conclusion

Petrographical and electron microprobe analysis of representative drill core samples of Petäjäskoski formation have yield the following results

- Petäjäskoski formation have mixed siliciclastic-carbonate sequence mostly made up of mudstone, with interlayered sandstone, and dolomite.
- The presence of phlogopite and sericite along with chlorite in mudstone and sandstone suggest these rocks have gone through lower greenschist facies metamorphism.
- Mudstone typically shows rhythmic fine dark and light coarse-grained layers, flaser bedding mostly made up of phlogopite, sericite, quartz, feldspar, and calcite rosette. One sample is typically chloritized with abundant chlorite, pyrite, epidote, and calcite.
- Sandstone occurs as three distinct types one is recrystallized carbonate rich sandstone with quartz, feldspar, chlorite, biotite and muscovite with trace zircon, and hematite.
- The second sandstone type is in form of sericite sandstone deformed and altered containing abundant pseudomorphs after anhydrite/gypsum due to replacement of evaporitic minerals by calcite. The other minerals include quartz, feldspar (Plagioclase, orthoclase), muscovite trace rutile floating in sericite and argillaceous matrix.
- The third sandstone is completely distinct from other lithologies petrographically as sub-arkose sandstone with well-rounded quartz and greater than 25% feldspar as plagioclase, microcline and orthoclase and little calcite, biotite, chlorite, zircon, and hematite.
- Dolomite is coarse grained recrystallized dolomite with xenotopic texture having talc, quartz.
- Breccia are monomictic conglomerate consist of rounded clasts of mudstone along with feldspar and quartz, talc, with sericite cement.
- Electron microprobe studies for selected samples yields trace quantity of halite, anhydrite, bischofite, and sylvite in sandstone.
- Trace quantity of these evaporite minerals along with micro-textures like anhydrite pseudomorphs, fractures filled calcite replacements of anhydrite and calcite rosette clearly depicts the evaporitic origin of Petäjäskoski formation, thus making these rocks the oldest occurrence of evaporites in Fennoscandian shield

- Petäjäskoski formation was a shallow ramp tidal flat or lagoonal sequence based on trace amount of halite, bischofite, sylvite, and anhydrite in microprobe studies, pseudomorphs of anhydrite, calcitization of evaporites in fractures, calcite rosette, sedimentary structures like flaser bedding in mudstone, cross bedding in sandstone, stromatolites in dolomite, where to some extent depositional conditions were favorable for formation of evaporites, which in turn is postulated by extensive albitization, carbonatization, chloritization and solution collapsed breccias in Paleoproterozoic rocks of Peräpohja belt.

9. References

Adnan, A., Shukla, U.K., Verma, A., Shukla, T., 2015. Lithofacies of transgressive–regressive sequence on a carbonate ramp in Vindhyan basin (Proterozoic): a case of tidal-flat origin from central India. Arabian Journal of Geosciences, 8(9), pp. 6985–7001.

Davey, J., 2019. Anomalous metal enrichment of Basin Brines in the Zambian Copperbelt: A comparison of fluid chemistry in contrasting sediment-hosted copper systems. University of Southampton, Doctoral Thesis, 250pp.

Frietsch, R., Tuisku, P., Martinsson, O., Perdahl, J. A., 1997. Early proterozoic Cu-(Au) and Fe ore deposits associated with regional Na-Cl metasomatism in northern Fennoscandia. Ore Geology Reviews, 12(1), 1–34.

Győri, O., Haas, J., Hips, K., Lukoczki, G., Budai, T., Demény, A., Szőcs, E., 2020. Dolomitization of shallow-water, mixed silicilastic-carbonate sequences: The Lower Triassic ramp succession of the Transdanubian Range, Hungary. Sedimentary Geology, 395, 105549.

Huhma, H., Cliff, R. A., Perttunen, V., Sakko, M., 1990. Sm-Nd and Pb isotopic study of mafic rocks associated with early Proterozoic continental rifting: the Peröpohja schist belt in northern Finland. Contributions to Mineralogy and Petrology, 104(3), 369–379.

Hanski, E., Huhma, H., Perttunen, V., 2005. SIMS U-Pb, Sm-Nd isotope and geochemical study of an arkosite-amphibolite suite, Perapohja Schist Belt: evidence for ca. 1.98 Ga A-type felsic magmatism .Geological Society of Finland, Bulletin *77*(1), 5.

Hanski, E., Huhma, H., Vuollo, J., 2010. SIMS zircon ages and Nd isotope systematics of the 2.2 Ga mafic intrusions in northern and eastern Finland. Geological Society of Finland, Bulletin 82, pp 31–62.

Hölttä, P., Heilimo, E., 2017. Metamorphic map of Finland. In: Nironen, M. (Ed.) Bedrock of Finland at the scale 1:1 000 000 – Major stratigraphic units, metamorphism and tectonic evolution Guide to the Geological Map of Finland – Bedrock 1:1 000 000. Geological Survey of Finland, Special Paper 60, 75-126.

Haverinen, J., 2020. Evaporites in the Central Lapland Greenstone Belt. MSc Thesis. University of Helsinki, p. 80p.

Iljina, M., & Hanski, E. 2005. Layered mafic intrusions of the Tornio-Näränkävaara belt. In: lehtinen, M., Nurmi, P.A., Rämö, O.T (Eds), Precambrian geology of Finland- key to evolution of Fennoscandia shield. Elsevier B.V, Amsterdam, pp 101-138.

Karhu, J.A., 1993. Paleoproterozoic evolution of the carbon isotope ratios of sedimentary carbonates in the Fennoscandian Shield. Geological Survey of Finland, Bulletin 371, p. 87.

Karhu, J., Kortelainen, N., Huhma, H., Perttunen, V., Sergeev, S., 2007. New time constraints for the end of the Paleoproterozoic carbon isotope excursion. In 7th Symposium on Applied Isotope Geochemistry, Steelenbosch, South Africa, 10th–14th September, 2007, Abstracts (pp. 76-77).

Köykkä, J., Lahtinen, R., Huhma, H., 2019. Provenance evolution of the Paleoproterozoic metasedimentary cover sequences in northern Fennoscandia: Age distribution, geochemistry, and zircon morphology. Precambr. Res. 331, 105364

Kyläkoski, M., Hanski, E., Huhma, H., 2012. The Petäjäskoski Formation, a new lithostratigraphic unit in the Paleoproterozoic Peräpohja Belt, northern Finland. Bull. Geol.Soc.Finland 84(2), 85-120.

Keays, R. R. (1995). The role of komatiitic and picritic magmatism and S-saturation in the formation of ore deposits. *Lithos*, *34*(1-3), 1-18.

Lahtinen, R, Sayab, M., Karell, F., 2015. Near-orthogonal deformation successions in the poly-deformed Paleoproterozoic Martimo belt: Implications for the tectonic evolution of Northern.Precambr Research. 270, 22-38

Lahtinen, R, Huhma, H., Lauri, L.S., Sayab, M., 2019. Geochemical and U-Pb and Sm-Nd isotopic constraints on the evolution of the Paleoproterozoic Ylitornio nappe complex, northern Fennoscandia.bulletin Geological Society of Finland 91(1), 75-100.

Li, C., Ripley, E. M., Naldrett, A. J., Schmitt, A. K., & Moore, C. H., 2009. Magmatic anhydrite-sulfide assemblages in the plumbing system of the Siberian Traps. Geology, 37(3), 259–262.

McPhie, J., Kamenetsky, V. S., Chambefort, I., Ehrig, K., Green, N., 2011. Origin of the supergiant Olympic Dam Cu-U-Au-Ag deposit, South Australia: Was a sedimentary basin involved? Geology, 39(8), 795–798.

Melezhik, V. A., Fallick, A. E., Rychanchik, D. V., & Kuznetsov, A. B., 2005. Palaeoproterozoic evaporites in Fennoscandia: implications for seawater sulphate, the rise of atmospheric oxygen and local amplification of the δ13C excursion. Terra Nova, 17(2), 141-148.

Melezhik, V., Prave, A. R., Hanski, E. J., Fallick, A. E., Lepland, A., Kump, L. R., Strauss, H., (Eds.), 2012. Reading the Archive of Earth's Oxygenation: Volume 3: Global Events and the Fennoscandian Arctic Russia-Drilling Early Earth Project.

Melezhik, V. A., Bingen, B., Sandstad, J. S., Pokrovsky, B. G., Solli, A., Fallick, A. E., 2015. Sedimentary-volcanic successions of the Alta–Kvænangen Tectonic Window in the northern Norwegian Caledonides: Multiple constraints on deposition and correlation with complexes on fennoscandian shield. Norw. J. Geol. 95, 245-284.

Molnár, F., Oduro, H., Cook, N. D. J., Pohjolainen, E., Takács, Á., O'Brien, H., Pakkanen, L., Johanson, B.o., Wirth, R., 2016. Association of gold with uraninite and pyrobitumen in the metavolcanic rock hosted hydrothermal Au-U mineralisation at Rompas, Peräpohja Schist Belt, northern Finland. Mineralium Deposita, 51(5), 681–702.

Niiranen, T., Hanski, E., Eilu, P., 2003. General geology, alteration, and iron deposits in the Palaeoproterozoic Misi region, northern Finland.

Perttunen, V., Hanski, E., 2003. Pre-Quaternary rocks of the Törmäsjärvi and Koivu map-sheet areas. Explanation to the Maps of Pre-Quartenary Rocks, Sheets, 2631. Geological Survey of Finland.

Piippo, S., Skyttä, P., Kloppenburg, A., 2019. Linkage of crustal deformation between the Archean basement and the Proterozoic cover in the Peräpohja area, northern Fennoscandia. Precambr. Res. 324, 285–302.

Pirajno, F., Cawood, P. A., 2009. Hydrothermal processes and mineral systems. Geological Survey of Western Australia.

Ranta, J.-P., Lauri, L. S., Hanski, E., Huhma, H., Lahaye, Y., Vanhanen, E., 2015. U–Pb and Sm–Nd isotopic constraints on the evolution of the Paleoproterozoic Peräpohja Belt, northern Finland. Precambrian Research, 266, 246–259.

Ranta, J.-P., Molnar, F., Hanski, E., Molnár, F., Cook, N., 2018. Epigenetic gold occurrence in a Paleoproterozoic meta-evaporitic sequence in the Rompas-Rajapalot Au system, Peräpohja belt, northern Finland. Bull. Soc. Finland 90 (1), 69-108.

Rose, A. W., 1976. The effect of cuprous chloride complexes in the origin of red-bed copper and related deposits. Economic Geology, 71(6), 1036-1048.

Saintilan, N. J., Selby, D., Creaser, R. A., Dewaele, S., 2018. Sulphide Re-Os geochronology links orogenesis, salt and Cu-Co ores in the Central African Copperbelt. Scientific reports, 8(1), 1-8.

Selley, R. C., 2000. Applied sedimentology. 523.

Tuisku, P., 1986. The origin of scapolite in the Central Lapland schist area, Northern Finland; preliminary results. Bulletin-Geological Survey of Finland, (331), 159-173.

Tapio, J., Ranta, J. P., Cook, N., Lahaye, Y., O'Brien, H., 2021. Paleoproterozoic Rajapalot Au-Co system associated with evaporites: Chemical composition and boron isotope geochemistry of tourmaline, and sulfur isotopes of sulfates, Peräpohja belt, northern Finland. Precambrian Research, 365, 106410.

Warren, J.K., 2016. In: Evaporite, a Geological Compendium, 2nd ed. Springer, Switzerland, p. 1822.

Wilde, A. R., Layer, P., Mernagh, T., Foster, J., 2001. The giant Muruntau gold deposit: geologic, geochronologic, and fluid inclusion constraints on ore genesis. Economic Geology, 96(3), 633-644.

Yantambwe, M. I., Cailteux, J. L. H., 2019. Geological observations in the five-klippes area, northwestern katanga copperbelt (Democratic Republic of the Congo). Geologica Belgica, 22(3–4), 111–119.

Yardley, B. W., Cleverley, J. S., 2015. The role of metamorphic fluids in the formation of ore deposits. Geological Society, London, Special Publications, 393(1), 117-134.